Electronic Thesis and Dissertation Repository

1-17-2022 10:00 AM

Development of a Tissue Specific Bioscaffold for Intestinal Stem Cell Culture

Sachin Kakar, *The University of Western Ontario*

Supervisor: Asfaha, Samuel., *The University of Western Ontario*
Co-Supervisor: Flynn, Lauren E., *The University of Western Ontario*
A thesis submitted in partial fulfillment of the requirements for the Master of Science degree in Pathology and Laboratory Medicine
© Sachin Kakar 2022

Follow this and additional works at: https://ir.lib.uwo.ca/etd

Part of the Laboratory and Basic Science Research Commons

Abstract

The generation of a tissue-specific intestinal hydrogel using small intestinal extracellular matrix (ECM) has the potential to support and promote the growth of intestinal organoids. In this study, we aimed to develop hydrogels derived exclusively from intestinal ECM or composites comprised of intestinal ECM combined with alginate, which may allow greater tuning of the hydrogel properties. A novel mouse intestinal decellularization protocol was developed and the ECM was characterized. Our analysis demonstrates that cellular and nuclear content was removed effectively, while preserving key ECM components. When decellularized ECM was used to generate hydrogels, the resulting ECM displayed bioactivity as demonstrated by metabolic and pro-proliferative effects on NIH 3T3 murine fibroblasts. More importantly, our novel ECM hydrogel also supported intestinal organoid growth. These studies demonstrate that tissue-specific ECM-derived hydrogels can indeed support and promote the growth of intestinal organoids *in vitro*.

Keywords

Summary for Lay Audience

The small intestine is the organ in the body where most food digestion and nutrient absorption takes place. It has been shown previously that stem cells give rise to all of the cell types in the intestine, which is important for normal tissue turnover and healing. Interestingly, these stem cells can be isolated from tissues and used to form "mini-intestines" in a petri dish, called organoids. These organoids may allow researchers to develop models of intestinal diseases for testing the effects of different drugs, or potentially could be used to develop cell-based therapies for regenerative medicine applications. Currently, the only way to form organoids is by encapsulating and culturing them within a jello-like material called Matrigel®, which contains essential proteins needed for the stem cells. However, Matrigel® is produced by mouse cancer cells, which means that the cells generated using this approach cannot be used for clinical applications. The purpose of this study was to develop new biomaterials to replace Matrigel® for the growth of organoids, using proteins sourced from intestinal tissues. There is evidence to support that such intestinal-derived materials could support the survival and growth of stem cells, and help them to give rise to the other cell types in the intestine. This thesis developed a new method for isolating intestinal-specific proteins from mouse tissues. Further, these proteins were further processed to enable the formation of gels that could be used to encapsulate cells. Cell culture studies confirmed that the intestinal protein gels supported cell viability and the growth of mouse intestinal organoids, similar to Matrigel®. In addition, the effects of combining the intestinal proteins with alginate, a natural gel that comes from seaweed, were explored to develop composite materials that had more tunable mechanical properties. While the organoids were successfully encapsulated and cultured within these composites, further studies are needed to refine the conditions to promote organoid growth. Overall, this thesis contributed to the development of promising new biomaterials that hold the potential to replace Matrigel® as a more clinically translational tissue-specific platform for studies of intestinal organoids.

Co-Authorship Statement

Liyue Zhang	Helped with culturing organoids in Matrigel® and provided R-spondin for the cultures.
Courtney Brooks	Helped with developing a working protocol for the MTT assay.

All data presented in the figures was collected by Sachin Kakar.

Acknowledgments

I would first like to thank my supervisors Dr. Asfaha and Dr. Flynn for their endless support and guidance throughout my MSc. Thank you for all the patience and confidence you provided me in my work.

I would like to thank all the members of the Asfaha and Flynn lab, past and present, for their help and support throughout my MSc. Specifically, I'd like to thank Liyue Zhang and Courtney Brooks for their assistance with learning many laboratory techniques. I am also grateful for the support and friendships provided over the past two years from my fellow lab mates including John Walker, Julia Terek, and McKenna Tosh.

I would like to thank Dr. Dagnino who generously donated NIH 3T3 cells. I would also like to thank Sheradan Doherty for her generous donation of decellularized meniscus.

To my advisory committee, Dr. Dean Betts and Dr. Douglas Hamilton, thank you for your continuous feedback and guidance that brought this project to completion.

Thank you to my friends, especially Ricky Tristan, for always lifting me up and providing me with continuous support and confidence.

Thank you to Saina Goswami for your love, support, and time throughout my MSc and for always brightening my days.

Special thanks to my family, especially my parents, Ashwani and Vimi, for your love and support throughout my education. All my successes are dedicated to you, as they would not have been possible without you.

Table of Contents

List of Figures

List of Appendices

List of Abbreviations

2D	Two-dimensional
3D	Three-dimensional
ABAM	Antibiotic- antimycotic
BMP	Bone morphogenic protein
DAPI	4',6-diamidino-2-phenylindole
dH$_2$O	Deionized water
DM	Decellularized meniscus
DMMB	Dimethylmethlyene blue
DNase	Deoxyribonuclease
dsDNA	Double-stranded DNA
DSI	Decellularized small intestine
ECM	Extracellular matrix
EDTA	Ethylenediaminetetraacetic acid
EGF	Epidermal growth factor
GAG	Glycosaminoglycan
H&E	Hematoxylin and eosin
HBSS	Hank's balanced salt solution
hPSC	Human pluripotent stem cell

IHC	Immunohistochemistry
ISC	Intestinal stem cell
ISEMF	Intestinal subepithelial myofibroblasts
LGR5	Leucine-rich repeat-containing G protein-coupled receptor 5
MMP	Matrix metalloproteinase
PBS	Phosphate buffered saline
PEG	Polyethylene glycol
PMSF	Phenylmethylsulfonyl fluoride
RGD	Arginine-glycine-aspartate
RNase	Ribonuclease
S.D	Standard deviation
SDS	Sodium dodecyl sulphate
sGAG	Sulphated Glycosaminoglycan
SPB	Sorenson's phosphate buffer
TBST	Tris-buffered saline with 0.1% tween
TCPS	Tissue culture polystyrene
TE	Tris-EDTA
Wnt	Wingless-related integration site
YAP	Yes-associated protein 1

Chapter 1

1   Literature Review

1.1   Small Intestine

1.1.1 Structure and Function

The small intestine or small bowel is a luminal organ that connects the stomach and large bowel. The length of the small intestine is variable, but on average is estimated to be between 3 to 5 meters[1]. Functionally, the small intestine plays a vital role in the digestion and absorption of nutrients[1,2]. This tube-shaped organ is comprised of three main structural parts: the duodenum, jejunum, and ileum (Figure 1.1).
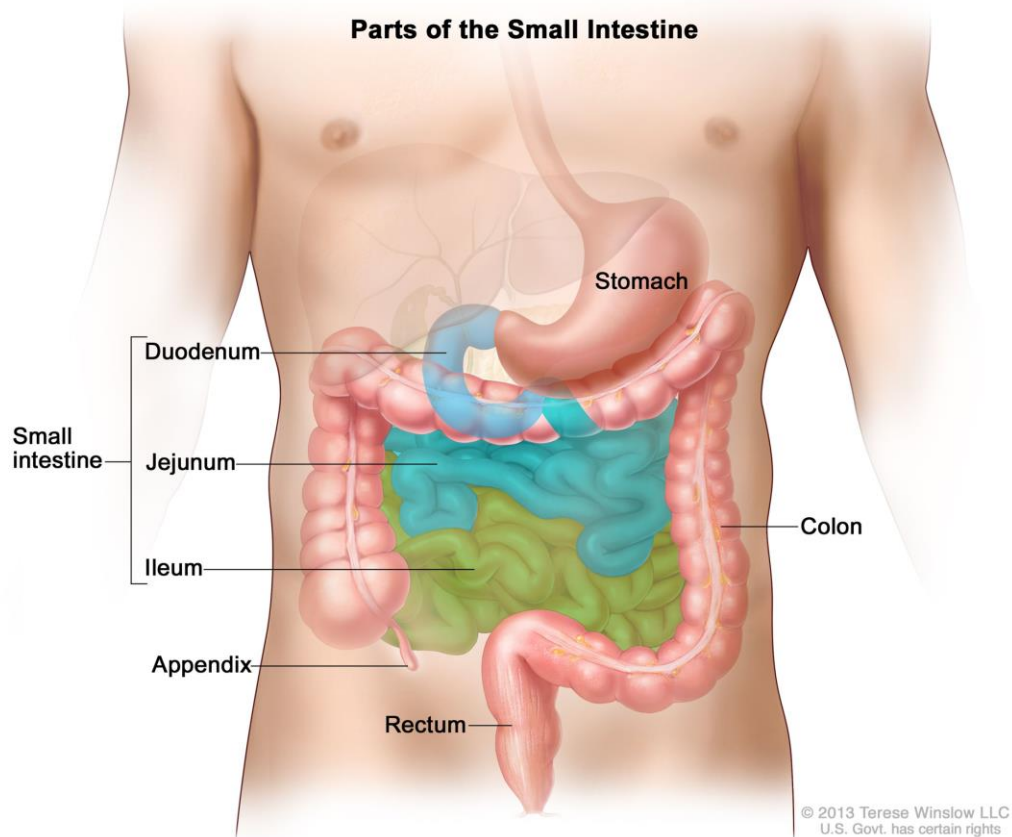
Figure 1.1. Anatomy of the small intestine. Diagram showing the parts of the small intestine including the duodenum, jejunum, and ileum, and surrounding structures. Image obtained with permission from Terese Winslow.

The duodenum is the first and shortest segment of the small intestine. It connects to the pylorus of the stomach at its proximal end and the jejunum at its distal end[1–3]. The role of the duodenum includes receiving partially-digested food (chyme) from the stomach and chemically digesting the chyme in preparation for absorption within the small intestine. As the duodenum processes chyme, it also absorbs some nutrients, the most notable of which is iron[1–3]. The jejunum, on the other hand, begins at the suspensory muscle of the duodenum (ligament of Treitz) and forms the middle portion of the small intestine. The jejunum is where important nutrients such as carbohydrates, protein, fat, and vitamins are absorbed. These absorbed nutrients can then enter the bloodstream where they can be further distributed to other organs within the body[1–3]. The ileum is the third and final segment of the small intestine and is where remaining nutrients are absorbed including vitamin B12 and bile acids[1–3].

1.1.2 Intestinal Cell Populations

The intestinal lining is comprised of a single cell layer of intestinal epithelial cells that line the luminal surface. The lining itself is organized in a structure that includes fingerlike projections called villi and invaginations known as crypts (Figure 1.2). The epithelial cells play a vital role in the digestion of food and the absorption of nutrients, as well as protecting the human body from infection[4]. Importantly, the epithelium continually renews itself every 3-5 days, with new epithelial cells being produced by stem cells, which are located at the base of the crypts[1,3]. Progenitor cells derived from these stem cells give rise to subsets of cells that ultimately differentiate into either secretory or absorptive epithelial cells as they migrate up the crypt-villus axis[1–3]. The older epithelial cells undergo cell death and are brushed off into the intestinal lumen[3].
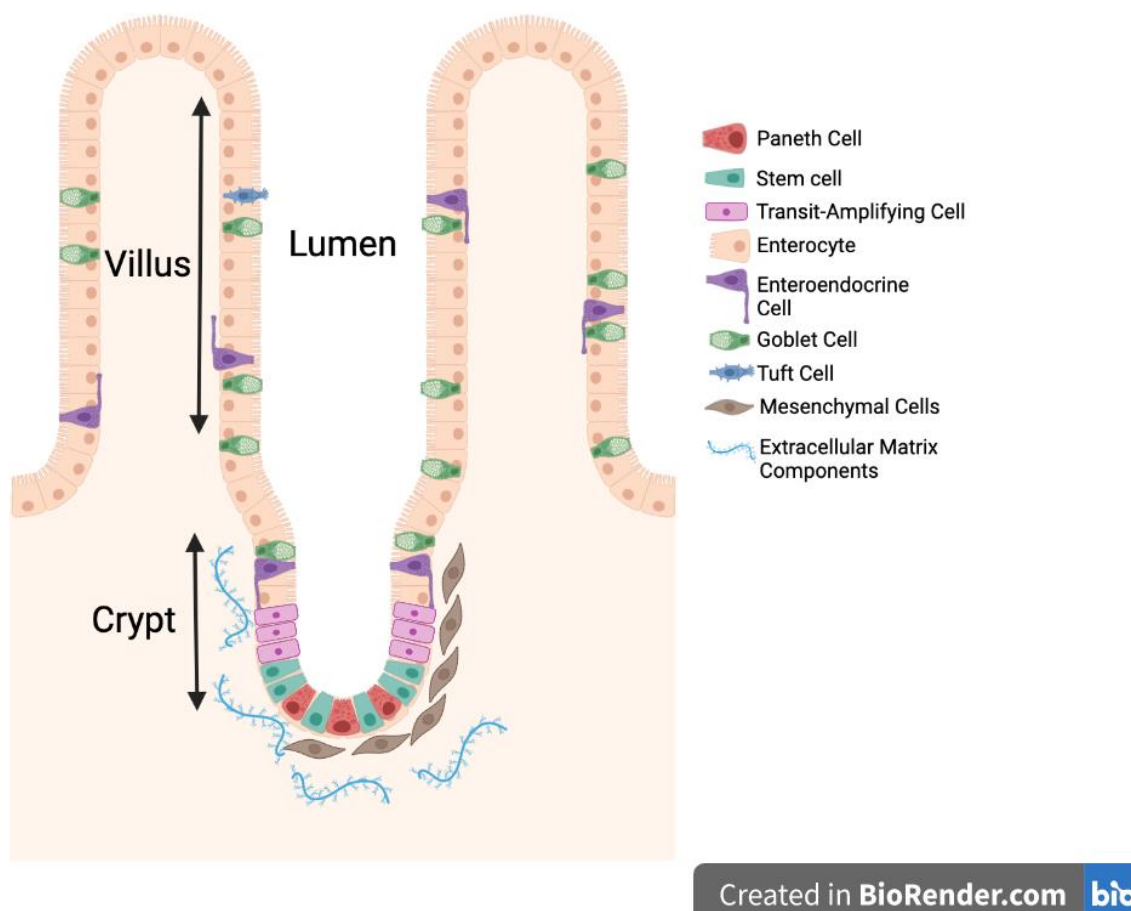
Figure 1.2. The structure of the intestinal epithelium. Stem cells located at the base of the crypts, surrounded by Paneth cells, mesenchymal cells, and an extracellular matrix (ECM), ultimately give rise to daughter cells. Daughter cells (transit-amplifying cells) differentiate into either absorptive (enterocytes) or secretory (Paneth, enteroendocrine, goblet, and tuft cells) cell types and migrate along the crypt-villus axis. Eventually, older cells at the tip of the villi undergo cell death and are brushed off into the lumen. The image was created in BioRender.com.

Within the epithelium, there are several cell types present including enterocytes, goblet cells, Paneth cells, endocrine cells, tuft cells and intestinal stem cells (ISCs). Enterocytes are columnar cells that primarily have an absorptive function for nutrients[5–7]. Goblet cells are columnar-shaped cells that secrete mucus to lubricate the intestinal wall for ease of passage of food and protection from digestive enzymes and pathogens[5]. Paneth cells are highly specialized cells specific to the small intestine, which provide niche factors and signals necessary for ISC homeostasis within the crypt base, and secrete antimicrobial peptides that protect against pathogens[1,2,4,5]. Endocrine cells can be found along the

crypt-villus axis of the intestinal mucosa. Their main function involves secreting hormones and releasing them into the bloodstream upon stimulation[6]. Tuft cells, also known as brush cells, are found along the crypt-villus axis. Although they act as chemosensory cells which can sense luminal content, their exact role in homeostasis is not fully understood[8,9]. ISCs reside at the crypt base alongside Paneth cells, and serve to give rise to all epithelial cells in the intestine. The intermediate daughter cells (transit-amplifying cells) derived from the ISCs proliferate and migrate along the crypt-villus axis, where they can differentiate into the different cell types of the intestine[7,10]. To maintain their self-renewal and differentiation potential, ISCs are surrounded by a cellular and physical niche that includes both epithelial and mesenchymal cell populations distributed throughout the intestinal extracellular matrix (ECM)[7].

1.1.3 Intestinal Extracellular Matrix

The ECM of the small intestine is a complex network of proteins and polysaccharides that forms the supporting structure for the intestinal epithelium while also providing essential biochemical cues[7]. The ECM surrounding the intestinal crypts incorporates numerous bioactive proteins including laminin, various types of collagen, proteoglycans, and fibronectin[7].

Collagens: Collagen is the most abundant protein in the body and is the primary structural protein in the ECM[11]. Collagen's triple-helical structure allows it to assemble into molecular complexes such as networks, which provide structural support to the ECM[11–13]. In the healthy small intestine, the collagen fibers are organized in a cross-cross pattern[14]. In addition to the structural role of collagen, collagens in the ECM are also known to play bioactive roles by regulating cell adhesion, cell migration, and directing tissue development[12]. Collagen subtypes I, III, IV, and VI are found well distributed throughout the ECM of the small intestine[7]. Studies suggest that collagen VI is a key regulator of the microenvironment for intestinal epithelial crypt cells[7,15]. Collagen VI is known to interact with type IV collagen found in the basement membrane that is in direct contact with the intestinal epithelial cells. Abnormalities in the structure and distribution of collagen fibers can occur in intestinal diseases[14]. Changes in the collagen content

within tissues can impact tissue stiffness, which in turn can regulate cellular processes including growth factor signaling and cytoskeletal contractility[16–18].

Laminin: Laminin is an abundant glycoprotein found in the ECM of the intestinal crypts, and plays an important role in regulating intestinal epithelial cell function[7,19]. This cross-shaped molecule is made up of three polypeptide chains that allow for the formation of self-assembled laminin networks[20]. Laminin can also interact with other ECM molecules, such as collagen[20]. Laminin expression during early development suggests that it plays an important role in cell differentiation in the epithelium[21]. Cells interact with laminin through cell surface receptors known as integrins. Functionally, interactions with laminin can modulate cellular activities including cell adhesion, migration, and survival[21,22]. Alterations in laminin distribution and expression have been detected in various pathologies of the intestine, emphasizing its importance in regulating cell function[7,23].

Fibronectin: Fibronectin is an ECM glycoprotein found in all tissues that is an important mediator of cell-matrix interactions. Fibronectin assembles into a fibrillar matrix through cell-mediated processes[18]. The fibronectin fibrils can form linear or branched networks that function to interconnect neighbouring cells, and it has both structural and functional roles within tissues[18]. Fibronectin has domains that allow it to interact with other proteins and glycosaminoglycans found within the ECM, as well as with cell surface receptors[7,24,25]. Intestinal fibronectin is secreted by both fibroblasts and epithelial cells[26,27]. Similar to other basement membrane proteins, irregular deposition patterns of fibronectin have been correlated with various intestinal pathologies[7,26,28].

Glycosaminoglycans: Glycosaminoglycans (GAGs) are carbohydrate molecules that have important biologic functions. GAGs are covalently attached to core proteins to form proteoglycans[12] and can interact with other proteins to regulate cell signaling, cell proliferation, and angiogenesis[29,30]. GAGs can be divided into two main types: (i) non-sulphated GAGs, such as hyaluronic acid, or (ii) sulphated GAGs (sGAG), such as chondroitin sulphate and heparan sulphate[30]. GAGs are important for both lubrication and structural support within the intestinal ECM[30]. In the small intestine, heparan sulphate

and hyaluronic acid play a role in signaling pathways that regulate embryonic development, tissue homeostasis, intestinal crypt homeostasis, and inflammation[31–35].

Overall, the intestinal ECM is essential for the growth of epithelial cells *in vivo.* More recently, it has been discovered that the ECM can be used to support the growth of ISCs *in vitro*[36].

1.2   Intestinal Organoid "mini-guts"

1.2.1   Overview of Intestinal Organoids

Over the last decade, an increasing number of studies have grown either single or clusters of epithelial cells in substances that contain components of the basement membrane, primarily Matrigel®, to form tissue-resembling structures known as organoids. Culturing within a three-dimensional (3D) microenvironment that mimics the *in vivo* milieu provides cells with cues that stimulate their self-organization to form "mini-guts", in contrast to the monolayer culture that is typically observed when the cells are expanded in two-dimensional (2D) cell culture models[37]. Organoids recapitulate features of the native small intestine from an anatomic, cellular, and functional basis[38]. More specifically, intestinal organoids contain a functional lumen that is surrounded by a polarized epithelial layer (Figure 1.3). This layer has all of the cell types of the epithelium organized with similar proportions of cell types as what is found in the native organ[39]. *In vitro* studies have evaluated the use of intestinal organoids for testing epithelial permeability to a variety of molecules, validating their use as a potential *in vitro* drug transport model[40]. Organoids have also been applied to model intestinal diseases caused by inflammation or physical injuries, such as inflammatory bowel disease, Crohn's disease, short bowel syndrome, and colorectal cancer[40].
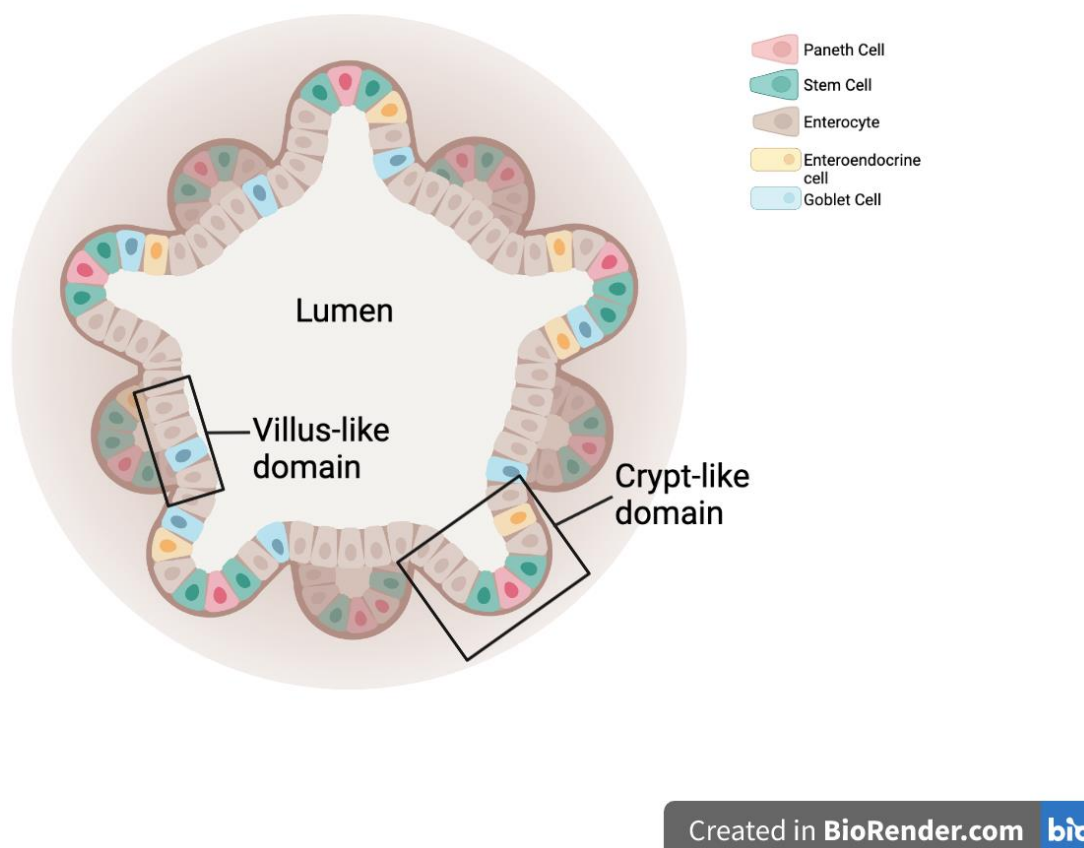
Figure 1.3. Intestinal organoid morphology. An epithelial monolayer with budding crypt-like domains surrounds a central lumen. Stem cells and differentiated cell types found along the epithelial monolayer eventually undergo cell death and are brushed off into the lumen. Image was created in BioRender.com.

1.2.2   Current Methods for Generating Organoids

Intestinal organoids can be derived from primary intestinal tissue or from pluripotent stem cells[40].

Primary Tissue-Derived Organoids: Organoids derived from primary intestinal tissues were first described by Hans Clevers' group in 2009[36]. More specifically, the authors described a culture system in which a single stem cell characterized by its expression of leucine-rich repeat-containing G protein-coupled receptor 5 (LGR5), was able to give rise *in vitro* to crypt-villus structures, without the addition of a mesenchymal component[36]. The initial protocol that was published by Sato *et al.* described a methodology that could be used to isolate mouse intestinal crypts and subsequently culture them to form

organoids[41]. In this system, primary intestinal tissues were embedded in Matrigel® and cultured in media supplemented with growth factors, including R-Spondin-1, epidermal growth factor (EGF), and Noggin. These factors are a wingless-related integration site (Wnt) signaling agonist, an inducer of intestinal proliferation, and a bone morphogenic protein (BMP) inhibitor, respectively[36,42–44]. These adult stem cell-derived intestinal organoids are characterized by an epithelial monolayer that surrounds a hollow lumen. The epithelial cells in these organoids are known to contain all of the cell types found *in vivo*, including stem cells and cells important for the ISC niche such as Paneth cells[36,45]. In addition to developing this culture system for the mouse small intestine, researchers have further adapted these protocols to grow organoids from human small intestine and both human and mouse colon[36,41].

Pluripotent Stem Cell-Derived Organoids: Building on the organoid cultures established by the Clevers group, new protocols for generating human intestinal organoids from human embryonic and induced pluripotent stem cells have also been developed[46,47]. Using various growth factors, robust processes have been established to direct the differentiation of human pluripotent stem cells (hPSC) into intestinal cells[46]. When cultured within Matrigel® in the presence of inductive growth factors that promote cell differentiation, the pluripotent stem cells can form 3D organoids that have a polarized epithelium that contains the various cell types found *in vivo*[39,46,47]. In contrast to organoids derived from primary intestinal tissues, these pluripotent stem cell-derived organoids also incorporate a mesenchymal component that contributes to the signaling required for organoid growth[39].

1.3   Biomaterials for Intestinal Cell Culture and Delivery

1.3.1   Design Requirements

The formation of organoids requires the use of cell-supportive scaffolding materials that can encapsulate cells with high viability, forming a 3D niche in which the cells can adhere, grow, and differentiate[48]. The bioscaffold should provide biochemical cues that mimic the native ECM and needs to promote ISC proliferation and lineage-specific differentiation, while allowing the cells to self-organize into the organoid structures[48]. In

addition to bioactivity, the physical properties of the scaffolds can be important for generating organoids through ISC expansion[49]. In particular, the stiffness and porosity of the materials can affect the growth and differentiation of the ISCs[50]. Therefore, a material with tunable mechanical properties must be considered for an ISC culture system. Furthermore, an initial qualitative assessment of organoid growth is typically achieved by brightfield imaging of the 3D scaffold that encapsulates the organoids[36,50]. Therefore, having an optically clear or transparent material is vital for imaging at different depths by microscopy. As such, studies have focused on the use of natural biomaterials, which offer the advantage of providing innate bioactive cues, along with synthetic or semi-synthetic materials that have more tunable mechanical properties[48–50].

1.3.2   Matrigel®

Matrigel® is a soluble basement membrane protein extract derived from Engelbreth–Holm–Swarm mouse sarcoma cells[51]. Matrigel® has been used for decades in a variety of cell-culture applications, as it supports cell morphogenesis, differentiation, and promotes organoid assembly. Matrigel® is composed primarily of four major ECM proteins: laminin, collagen IV, entactin, and heparan sulphate. In addition to providing a bioactive microenvironment that regulates cell behavior, these proteins play a structural role in Matrigel®, allowing it to form a hydrogel at temperatures ranging from 22 to 37 °C[51,52]. To date, most ISC cultures have relied on Matrigel®, and it is currently the "gold standard" material for promoting intestinal organoid growth[48–50]. Matrigel®, however, has many limitations including that it is tumour-derived, its composition is ill-defined, it lacks tunability in its mechanical properties, and there can be batch-to-batch variability that may lead to reproducibility issues in cell culture experiments[51,52]. These limitations have led scientists to work on developing alternative scaffolds for intestinal cell culture and delivery.

1.3.3   Hydrogels

Hydrogels are 3D networks of hydrophilic polymers which have the ability to swell and retain large quantities of water without disrupting their structure due to polymer crosslinking[53]. Hydrogels can be formed physically or chemically, where physical gels

are stabilized through physical interactions and entanglement of the individual polymer chains, while chemical hydrogels are formed through covalent bonds[53,54]. Hydrogel crosslinking can be stimulated through a range of physical and chemical mechanisms including changes in temperature, pressure, and/or pH, exposure to light, or through their own chemical composition[53].

Hydrogels derived from natural materials, including components of tissues, are promising for cell culture and delivery applications due to their innate bioactivity and the fact that they can often be degraded through cell-mediated mechanisms[55]. Relative to hydrogels derived from synthetic polymers such as polyglycolic acid and polyethylene glycol (PEG), naturally-derived hydrogels tend to have weaker and less easily tuned mechanical properties but contain natural bioactive cues that help to support cell survival and function[55]. In the intestinal stem cell field, a variety of hydrogels and hydrogel composites have been investigated for applications in organoid growth and tissue regeneration[56–59]. In particular, alginate has been widely-investigated as a biomaterial due to its capacity to reversibly encapsulate cells and support their long-term viability in culture[60]. In addition, there is growing interest in the application of ECM-derived hydrogels sourced from decellularized small intestine to generate tissue-specific platforms, which will be discussed in detail in the next section.

Alginate Hydrogels: Alginate is a natural polymer derived from the walls of brown seaweeds, which is a polysaccharide comprised of β-(1–4) linked d-mannuronic acid and β-(1–4)-linked l-guluronic acid units[61]. Alginate possesses a range of desirable characteristics as a cell culture platform including controllable porosity, ease of gelation, and biodegradability[60]. Alginate crosslinks under mild conditions with the addition of divalent cations such as calcium and has been shown to support the viability of encapsulated cell populations[59–61]. Additionally, the crosslinking of alginate can be reversed to release cells with the use of chelating agents such as sodium citrate[62]. Alginate gels have previously been used in a range of applications including as cell culture platforms, wound dressings, drug delivery systems, and as an injectable gel for tissue-engineering applications[60,63]. One study by Capeling and colleagues demonstrated the use of alginate to support the growth of hPSC-derived intestinal organoids[59]. More

specifically, this study showed that human intestinal organoids grown on alginate were similar to human intestinal organoids grown on Matrigel®. Specifically, hPSCs were first cultured in Matrigel® before being encapsulated within alginate and crosslinked with calcium chloride. Using a LIVE/DEAD stain, they assessed spheroid viability on days 3 and 7 using different concentrations of alginate, and found that spheroids grown in 1% and 2% alginate remained nearly 100% viable, similar to Matrigel®. However, they found that the number of spheroids that gave rise to intestinal organoids on day 28 post-encapsulation was significantly lower in all alginate concentrations tested compared to Matrigel®. Histological and immunohistochemical analyses of the intestinal organoids at 28 days post-encapsulation revealed that the organoids grown in alginate expressed similar epithelial cell markers and proliferative cell markers with similar frequency to those grown in Matrigel®. Though hPSCs are distinct from primary mouse tissue, this study demonstrated promising evidence for the use of alginate-based platforms for the culture of intestinal cells.

1.4   Decellularized Tissue Bioscaffolds

1.4.1   Overview of Tissue Decellularization

Decellularization is a process that aims to isolate the ECM from native tissues and organs that can be used to develop tissue-specific bioscaffolds for cell culture and delivery[64]. The process involves the removal of cellular components that would induce an immunogenic response, while preserving the structure and composition of the native ECM as much as possible[65]. The extraction of cells requires methods that are unique to each tissue, tailored based on the physical and biochemical properties of the specific source[66]. The effectiveness of various methodologies used for decellularization depends on factors including the tissue cellularity, density, and lipid content[67]. Over the past two decades, virtually all tissue types have been decellularized including, but not limited to, the small intestinal submucosa, urinary bladder, adipose tissue, and bone[68–71]. Typically, decellularization protocols use a combination of physical, chemical, and enzymatic treatments selected to extract cells and cellular debris, while minimizing alterations to the structural components of the ECM[66].

Physical methods of tissue decellularization: Physical treatments may include agitation, the application of pressure, or freeze-thawing to promote cell lysis through the formation of ice crystals. All of these treatments result in the disruption of cell membranes and can assist in the removal of cell contents[64,66,67,72]. Though physical processing may be beneficial, these methods alone are not sufficient to extract cell contents from the tissues, and they are therefore commonly combined with chemical treatments to wash away the resultant cellular debris[66].

Chemical methods of tissue decellularization: Chemical treatment varies depending on the specific tissue undergoing decellularization. Hypertonic and hypotonic solutions are often used to lyse the cells within tissues through osmotic shock and are commonly used in combination with chelating agents such as ethylenediaminetetraacetic acid (EDTA) to disrupt cell-cell and cell-ECM interactions[66]. Treatment using ionic or non-ionic detergents is commonly employed to further solubilize cell membranes. Non-ionic detergents such as Triton-100X are thought to be favorable as they tend to have less of an impact on protein structure while still disrupting lipid-lipid and lipid-protein interactions[66]. Ionic detergents, such as sodium dodecyl sulphate (SDS) or sodium deoxycholate, are known to be stronger chemical agents that can be more effective at disrupting cell membranes, but can also cause changes in the native protein structure and composition[66,72]. Detergent treatments can also extract more soluble ECM components, including basement membrane constituents such as laminin, as well as GAGs[73]. In general, detergents need to be extensively washed away to avoid potential cytotoxic effects when the resultant bioscaffolds are applied in downstream studies[74].

Enzymatic methods of tissue decellularization: Enzymatic methods are often included in decellularization protocols, most typically proteases such as trypsin, nucleases such as deoxyribonuclease (DNase) and ribonuclease (RNase), and lipases[66]. Trypsin is a widely used enzyme in decellularization protocols as it disrupts integrin binding and releases cells from the ECM. However, prolonged exposure to trypsin can result in damage or loss of key ECM components including GAGs and laminin[66]. Residual nucleic acids remaining following cell lysis from physical and chemical treatments can be effectively degraded using nucleases such as DNase and RNase, and these are frequently

incorporated in decellularization protocols[64–67,72,75]. Enzymes, similar to detergents, need to be carefully rinsed away at the end of the tissue digestion process to avoid over-digestion or potential off-target effects.

1.4.2   Characterization of Decellularized Tissues

Following decellularization, it is important to characterize the tissues to confirm the removal of cellular components and the retention of key ECM components. A variety of methods can be used to assess and characterize decellularized tissues, however, there remains a need for improved guidelines on the amount of residual cellular debris that is acceptable when applying the scaffolds for cell culture or delivery[76,77].

Tissue decellularization is often evaluated using a combination of histological, immunohistochemical, and biochemical analyses. Nuclear content is often measured to detect the presence of residual cells and DNA[78,79]. Cell nuclei can be visualized in tissue sections through methods such as 4',6-diamidino-2-phenylindole (DAPI) staining, and double-stranded DNA (dsDNA) content can be quantified using the Quant-iT^{TM} Picogreen kit[80,81]. Aside from cellular content, the assessment of the structure and composition of the ECM is also important. Immunohistochemistry (IHC) can be used to visually assess the presence and distribution of ECM components in decellularized tissues[76]. Total collagen and sGAG content are often quantitatively assessed via the hydroxyproline assay and dimethylmethlyene blue (DMMB) assay, respectively[82–84]. Furthermore, picrosirius red staining can be performed to visualize the structure of the collagen fiber network, and toluidine blue staining is commonly employed to visualize the presence of GAGs[81,85]. More recently, techniques such as high-throughput mass spectrometry have allowed for a more detailed proteomic analysis of decellularized tissues[86,87].

1.4.3   Small Intestine Decellularization Protocols

With an interest in developing scaffolds for applications in intestinal tissue engineering, several groups have developed decellularization protocols for the small intestine and created bioscaffolds for intestinal cell culture[85]. A variety of animal models have been used as tissue sources, including rats, mice, and pigs[56,81,85]. Attempts have been made to

preserve the tissue architecture by leaving the entire intestine intact during processing, while in other cases, the tissue was minced to provide greater exposure to the decellularization agents and enhance cell removal[56,88]. Most decellularization protocols targeting the intestine have used harsh anionic detergents such as sodium deoxycholate or SDS. As discussed above, these detergents are effective at extracting cells, however, their use is also commonly associated with the loss of GAGs and denaturation of ECM proteins[56,67,74,81,85,88,89]. A smaller number of studies have employed non-ionic detergents such as Triton X-100, which have been shown to better preserve the ECM ultrastructure, while effectively removing cellular content[67,74,81,90]. In 2012, one study aimed to develop an intestinal decellularization protocol using a detergent-enzymatic treatment with rat intestine[85]. More specifically, the protocol used intact segments of the native intestine, which were treated with a solution of 4% sodium deoxycholate, followed by DNase. Following a single cycle of treatment, there was a significant reduction in DNA content and increased collagen content. With repeated treatment cycles, there was greater cell extraction but also a progressive loss of GAGs, along with disruption of the tissue ultrastructure based on scanning electron microscopy.

A study conducted by Oliveira *et al*. compared the use of different decellularization agents for mouse small intestine[81]. In particular, the study compared the use of varying concentrations of SDS (0.1% to 0.6%) or Triton X-100 (0.1% to 6%). Following treatment with SDS or Triton X-100 for 24 hours, they characterized cell removal and the retention of collagen and proteoglycans. Both methods significantly reduced the DNA content of the tissue as compared to native tissue controls. DNA quantification did not reveal any significant difference in levels of DNA between SDS-treated (8.63±4.06 ng of DNA per mg of dry weight of decellularized tissue) and Triton X-100-treated (9.70±14.05 ng/mg) small intestines. Semi-quantitative analysis of collagen fibers by picrosirius red staining intensity revealed that the SDS-treated intestines overall had significantly less collagen staining compared to native controls, whereas Triton X-100-treated groups showed similar staining intensities to the native controls. Semi-quantitative analysis of proteoglycan content determined by alcian blue staining intensity revealed no significant differences between the tissues treated with SDS or Triton X-100 compared to the native controls. All treated groups had alterations in the structural

organization of the ECM based on scanning electron microscopy images. However, samples treated with Triton X-100 were found to have a more well-preserved ECM structure as compared to SDS treated groups.

In another study in 2014, porcine small intestinal submucosa was decellularized using combined treatment with 1% SDS and 1% Triton X-100[74]. This protocol reduced the dsDNA content relative to native tissue samples (~64% decrease). However, cell culture studies using primary human esophageal smooth muscle cells showed reduced metabolic activity when the cells were cultured with the scaffolds, which was attributed to cytotoxic effects of residual detergent. This study additionally investigated the use of peracetic acid to decellularize the intestinal submucosa, but found there was no significant reduction in DNA content in the processed tissues relative to native controls[74].

Finally, a study in 2019 by Hans Clevers' group decellularized porcine small intestine using 4% sodium deoxycholate for 4 hours, followed by a washing step in Milli-Q water for 24 hours, and then DNase-I treatment for 3 hours[56]. Following decellularization, DNA was quantified using a DNA Mini Kit and measured using a Nanodrop. DNA content was significantly reduced in the decellularized tissue (~25 ng/mg) compared to native controls (~150 ng/mg). They further processed their ECM into a hydrogel and quantified their collagen and glycosaminoglycan contents. The relative collagen content in the decellularized samples (~27.81 μg/mg) was significantly higher compared to the native tissue samples (~13.92 μg/mg). Additionally, the glycosaminoglycan content was not significantly different in the decellularized samples (~0.51 μg/mg) as compared to native controls (~0.91 μg/mg).

1.4.4   ECM-Derived Scaffold Formats

ECM-derived bioscaffolds have been generated in a range of formats including foams, microcarriers, coatings, whole-organ scaffolds, and hydrogels, using a variety of different tissue sources to generate platforms tuned for cell culture and/or delivery[70,76,77,91,92]. In the context of the intestine, one study using decellularized rat small intestine attempted to preserve the entire small intestine-tissue architecture to generate 3D scaffolds for intestinal regeneration purposes[85]. Their tubular decellularized intestine was seeded with

amniotic fluid stem cells labeled with iron oxide particles by placing the labelled cells directly into the scaffold lumen. The researchers used magnetic resonance imaging (MRI) to investigate the distribution of the cells and found that cells were attached to the villus structure of the decellularized intestine. Additionally, using a chicken chorioallantoic membrane assay, they observed vessel growth towards their implanted decellularized tissues, suggesting their intestinal ECM may have pro-angiogenic effects[85]. Taking a similar approach, another study decellularized the porcine ileum and its associated vasculature, leaving the entire tissue architecture intact[89]. When their scaffolds were implanted subcutaneously in rats, they observed host cell infiltration starting at 2 weeks post-implantation and reported that there were no signs of an adverse immune response at up to 8 weeks post-implantation[89].

While preserving the 3D tissue architecture may be favorable for the design of tissue-engineered intestinal replacements, ECM-derived hydrogels that incorporate the complex composition of the ECM within a more tunable format that allows cell encapsulation are more appropriate as platforms for deriving intestinal organoids. As such, there is growing interest in the use of ECM-derived hydrogels for gastrointestinal organoid cultures and as injectable cell delivery systems for *in vivo* tissue regeneration applications[91,93]. Pepsin is the most widely-used enzyme for solubilizing tissue-derived ECM to generate peptide solutions that can be used to fabricate ECM hydrogels[57]. Hydrogels have been successfully produced from pepsin digests from a wide range of tissue sources including bone, cartilage, adipose tissue, and gastrointestinal tissues[56,57,94–98]. Notably, the pepsin digestion protocol must be carefully refined based on the properties of the specific tissue of interest. The enzymatic activity of pepsin and its effects on the ECM structure and composition are influenced by the digestion time, pH, concentration, and physical agitation[57]. Although pepsin cleaves proteins in many locations, protocols can be developed such that collagens are cleaved in locations where collagen fibril aggregates will unravel, without disrupting the collagen triple-helical structures required for ECM self-assembly into a hydrogel[56,57,99]. While pepsin digestion will alter the ECM structure and composition, hydrogels derived from pepsin-digested ECM have been shown to have bioactive effects on cells[56].

Some studies have used collagen-based gels for culturing intestinal cells[93-95]. For instance, a study in 2013 used hydrogels comprised of type I porcine tendon collagen to culture primary mouse small intestinal cells, both with and without the coculture of supporting intestinal subepithelial myofibroblasts (ISEMF), and compared to Matrigel® controls[100]. The collagen gels were able to support the growth of the murine small intestinal cells without coculture with ISEMF. However, morphological differences, particularly the lack of budding structures in organoids grown in collagen compared to Matrigel® were observed when the organoids were analyzed at 1 to 13 days post-culture. Additionally, epithelial expansion after 1 week in culture was significantly higher in Matrigel® as compared to the collagen gels. However, the collagen-based hydrogels were able to support the sub-culturing of the intestinal organoids for at least four passages[100].

Recently, Hans Clevers' group investigated the use of ECM hydrogels derived from decellularized porcine small intestine for culturing organoids from different endodermal tissues including the small intestine, liver, stomach, and pancreas[56]. Following decellularization, they solubilized their ECM using pepsin and subsequently used the solubilized ECM to form hydrogels that self-assembled at 37 °C. Proteomic analyses using mass spectrometry on the decellularized tissue prior to pepsin-digestion revealed that 749 proteins of 1600 identified were derived from either the ECM or extracellular exosomes. Additionally, fibrillar collagens such as types I, II, III, V and VI were the most abundant proteins identified. The ECM proteins identified were then clustered based on a publicly-available map of the human proteome, and they revealed a high degree of similarity in the composition of their ECM to tissues of endodermal origin including gut, pancreas, and liver. The porcine intestinal-derived hydrogels were shown to support the growth and viability of both human and mouse intestinal cells, which were characterized by brightfield imaging, histological analyses, as well as quantitative analyses of organoid diameter, similar to Matrigel®. However, the morphological quality of the human intestinal organoids was decreased after multiple passages in the intestinal-derived hydrogels.

1.4.5   Cell-Instructive Effects of the ECM

The composition, structure, and biomechanical properties of the ECM establish a microenvironment that regulates cell phenotype and function in a tissue-specific manner[77]. Cells interact with the ECM through cell surface receptors including integrins, which are proteins that facilitate cell-ECM adhesion[103]. Integrin binding can further regulate signaling pathways leading to the modulation of gene expression in cells[30,104]. In the context of the intestine, signaling regulated by integrin binding has been found to affect the maintenance of ISCs and the differentiation of epithelial cells[105,106]. For instance, β1 integrins have been implicated to be necessary for ISC proliferation by mediating the Hedgehog signaling pathway in mice[106]. The Hedgehog pathway is also involved in organogenesis and tissue repair in the intestine[30]. Basement membrane proteins and integrins have also shown differential expression along the crypt-villus axis in the human intestine[107–109]. For example, laminins with α1 heavy chains were found to be associated with differentiated cells in the villi, whereas the α2 variants were associated with the crypts[104,107]. Thus, the distribution of ECM components and integrin receptors in the intestine are tissue-specific and ultimately affect the fate of intestinal cells.

Although the native composition within ECM-derived scaffolds can influence cell behaviours via receptor-ligand interactions, degraded ECM products, termed matrikines, provide another potential mechanism through which the ECM can regulate cell behaviors[77,110]. Matrikines are generated through the enzymatic cleavage of extracellular proteins and proteoglycans by matrix metalloproteinases (MMPs). The fragmented molecules that are released as a result of proteolytic cleavage usually exert biological activities that differ from those of their full-length counterparts[110]. Studies have shown the production of matrikines to be associated with modulation of cell migration, adhesion, recruitment, and differentiation[77,111,112]. Interestingly, matrikines generated from GAGs have been shown to stimulate MMP production, which can subsequently act on remaining GAGs and promote the release of sequestered growth factors[77,110].

In addition to the biochemical properties of ECM-derived scaffolds, each tissue has unique biomechanical properties that can also influence cellular behaviour[113]. Cells can sense mechanical forces through the ECM through binding via integrins and formation of

cell adhesion complexes, which can lead to the activation of signaling cascades that influence cell adhesion, differentiation, and proliferation[77,105,114]. More specifically, biomechanical properties have been shown to play a critical role in controlling the self-renewal and lineage specification of ISCs[102,107].

A study by Gjorevski *et al.* in 2016 investigated the effects of matrix stiffness on ISC expansion[102]. The researchers encapsulated primary mouse ISCs in hydrogels composed of PEG and an Arg-Gly-Asp (RGD) peptide commonly found within ECM proteins. They quantified colony-forming efficiency and found that ISC proliferation was poor in matrices with soft stiffness (300 Pa), whereas ISC expansion was promoted when stem cells were encapsulated in hydrogels of intermediate stiffness (1.3 kPa). To investigate the mechanisms through which mechanical properties affect ISC expansion, they assessed the localization of yes-associated protein 1 (YAP) within the ISCs expanded in the hydrogels of varying stiffness. YAP is an effector of the hippo signaling pathway required for ISC self-renewal and expansion, and plays a role in cellular mechanosensing[30]. They found that YAP was primarily localized to the cytoplasm in the organoids encapsulated within soft hydrogels, whereas higher stiffness (1.3 kPa) hydrogels had higher nuclear localization after 1 day in culture. Thus, matrix stiffness was able to control ISC expansion through YAP-dependent mechanisms.

Despite the initial increase in YAP activity, the study found that the proportion of ISCs with YAP activity significantly dropped over time, leading them to investigate a dynamic matrix that could soften over time[102]. Instead of a static PEG hydrogel with a stable polymer (sPEG), they used a dynamic hydrolytically-degradable polymer (dPEG) that could soften over time. With the addition of RGD and laminin-111 in their hydrogels, they found that budding organoids could form in the dynamic matrices that softened over time and found differentiated cells and higher YAP activity in softening hydrogels compared to ones that remained stiff over time. Overall, the study demonstrated the importance of mechanical properties as they can affect signaling pathways necessary for both ISC expansion and differentiation. Other physical 3D architectural properties of the ECM can also influence cell behaviour[105]. In particular, parameters such as scaffold

porosity and surface topography of ECM-scaffolds can modulate cell-cell and cell-ECM interactions, and the binding of cells to the scaffolds[77,115].

1.5   Project Overview

1.5.1   Rationale

Currently, the "gold standard" for culturing intestinal organoids is Matrigel®, an ECM-derived product from mouse sarcoma cells. Matrigel® can support cell attachment and direct stem cell function including survival, proliferation, and differentiation. The need to culture in Matrigel®, however, remains a barrier to understanding the stem cell niche and characterizing its growth-promoting matrix proteins. The fact that Matrigel® is derived from mouse cancer cells limits the clinical utility of organoids grown using this culture system and Matrigel® could not be applied as an injectable cell delivery platform for therapeutic applications in humans. Recognizing these limitations, biomaterials derived from tissue-specific ECM represent a promising alternative for developing improved platforms for ISC culture and delivery. Specifically, hydrogels incorporating decellularized small intestine have the potential to enable cell encapsulation with high viability, similar to Matrigel®, while providing tissue-specific cues that may help to direct stem cell proliferation and differentiation.

1.5.2   Hypothesis

The overall objective of this project is to develop hydrogel biomaterials for cell encapsulation that incorporate intestinal-derived ECM that can be used in place of Matrigel® for the culture of intestinal stem cell-derived organoids. We hypothesized that the intestinal-derived ECM would provide cell-instructive cues that would modulate the response of encapsulated cell populations and promote intestinal organoid growth.

1.5.3   Specific Aims

Aim 1: To establish a decellularization protocol for mouse small intestine and characterize the resultant decellularized tissue.

Aim 2: To develop 3D hydrogels comprised exclusively of decellularized mouse small intestine and compare the response of encapsulated cell populations relative to Matrigel® controls.

Aim 3: To develop composite alginate-based hydrogels incorporating pepsin-digested decellularized mouse small intestine and confirm that the ECM has bioactive effects on encapsulated cell populations.

Chapter 2

2   Materials and Methods

2.1   Intestinal Decellularization

Adult male and female C57BL/6 mice (2–4 months in age) were euthanized by CO_2 overdose and the entire small intestine was surgically extracted by cutting at the pyloric sphincter and the ileocecal valve and subsequently transferred into Hank's balanced salt solution (HBSS). The intestines from ~35 to 45 mice were pooled together to create large batches and these were then perfused with HBSS using a needle and syringe to remove the intestinal contents. Next, the intestines were cut longitudinally with a scalpel, and scraped with a glass slide to remove any residual intestinal contents. Finally, the tissues were minced into ~2 mm pieces using surgical scissors.

For decellularization, all solutions were supplemented with 1% (v/v) antibiotic-antimycotic (ABAM) (Invitrogen, ON, Canada) and 0.27 mM phenylmethylsulfonyl fluoride (PMSF) (excluding enzymatic digestion steps) and all incubation steps were performed in a 100 mL solution volume at 37 ^{o}C under agitation on a Labnet 311DS orbital shaker control system (Labnet International, Inc., NJ, United States) at 120 rpm.

The tissues were subjected to three freeze-thaw cycles (-80 ^{o}C/ 37 ^{o}C, thawing at 120 rpm for 1-2 hours) in 10 mM tris (hydroxymethyl)aminomethane (Tris) and 5 mM ethylenediaminetetraacetic acid (EDTA) in deionized water (dH_2O) (pH 8.0). Solutions were replaced between each freeze/thaw cycle. After the third thaw, the samples were transferred into 50 mM Tris in dH_2O supplemented with 1% (v/v) Triton X- 100 (pH 8.0) for 24 hours. The samples were then rinsed three times for 20 minutes each in Sorenson's phosphate buffer (SPB) rinsing solution comprised of 0.55 M sodium phosphate dibasic heptahydrate ($Na_2HPO_4 \cdot 7H_2O$) and 0.17 M potassium phosphate (KH_2PO_4) in dH_2O (pH 8.0). The samples were then enzymatically digested for 6 hours in SPB digest solution comprised of 0.55 M $Na_2HPO_4 \cdot 7H_2O$, 0.17 M KH_2PO_4, and 0.049 M magnesium sulphate heptahydrate ($MgSO_4 \cdot 7H_2O$) in dH_2O (pH 7.3) supplemented with 300 U/mL deoxyribonuclease (DNase) Type II (from bovine pancreas) and 20 U/mL ribonuclease

(RNase) Type III (from bovine pancreas). Next, the samples were incubated in 1% (v/v) Triton X-100 in 50 mM Tris buffer (pH 8.0) for 24 hours. Finally, the samples were rinsed three times for 20 minutes in SPB rinsing solution, followed by two rinses in dH$_2$O for 30 minutes, and then frozen at -80 ºC and lyophilized using a Labconco Freezone 4.5 lyophilizer (Labconco, MO, United States) for 48 hours.

2.2 Compositional Characterization of the Decellularized Small Intestine

2.2.1 Histology

Native and decellularized small intestine (DSI) samples (n=3 cross-sections/batch, N=3 independent decellularization batches) were embedded in Tissue-Tek OCT compound (Sakura Finetek, CA, United States) and immediately placed on dry ice in preparation for cryosectioning (7 µm sections) with a Leica CM3050 S cryostat (Leica Microsystems Inc., ON, Canada). Samples were then fixed in acetone at -20 °C for 10 minutes, followed by three rinses in phosphate buffered saline (PBS) for 2 minutes each. Sections were stained with either (i) hematoxylin and eosin (H&E) to visualize the cells within the surrounding extracellular matrix (ECM), (ii) 4',6-diamidino-2-phenylindole (DAPI) in fluoroshield mounting medium (ab104139, Abcam) to visualize cell nuclei, (iii) picrosirius red to visualize collagen, or (iv) toluidine blue to visualize glycosaminoglycans (GAGs), following standard protocols. DAPI images were obtained using an EVOS FL fluorescence microscope (Thermo Fisher Scientific Inc., ON, Canada). H&E and toluidine blue staining was visualized using an EVOS XL Core microscope (Thermo Fisher Scientific Inc., ON, Canada), and the picrosirius red stained samples were imaged using a Nikon Optiphot polarizing microscope (Nikon Instruments Inc., NY, United States).

2.2.2 Biochemical Assays

Biochemical assays were performed to assess the composition of the DSI relative to native tissue controls. More specifically, the PicoGreen® assay was used to quantify the double-stranded DNA (dsDNA) content, collagen content was quantified using the hydroxyproline assay, and the dimethylmethyleneblue assay (DMMB) was used to

quantify the sulphated GAG (sGAG) content (N=7 independent decellularization batches for all assays).

Lyophilized samples were finely minced using surgical scissors in preparation for analysis. Ten mg of minced sample was then digested in 1 mL of Tris-EDTA (TE) buffer supplemented with 600 U Proteinase K (Qiagen, Germany) overnight at 56 $^{\circ}$C in a HERATherm Thermomixer oven at 1200 rpm (Thermo Fisher Scientific Inc., ON, Canada). The enzyme was inactivated by heating the samples to 92 $^{\circ}$C for 5 minutes while under agitation.

PicoGreen assay: Tissue samples were prepared using the DNeasy Blood & Tissue Kit (Qiagen, Germany), following the manufacturer's protocols. dsDNA content within the native and decellularized tissue samples was quantified using the Quant-iT**TM** PicoGreen® assay (Molecular Probes, Ontario). An eight-point standard curve ranging from 0 ng/mL to 500 ng/mL was prepared by serial dilution of the λ-DNA standard provided with the PicoGreen® kit in TE buffer. Fifty µL of each sample (diluted 1:20 for decellularized samples or 1:300 for native samples in TE buffer) was combined with 150 µL of Quant-iT™ reagent and fluorescence was read using a CLARIOstar® microplate reader, according to the manufacturer's instructions. The dsDNA concentration was normalized to the dry weight of each sample.

Hydroxyproline assay: A hydroxyproline assay was used to quantify the hydroxyproline concentrations within the decellularized and native tissue samples, as a measure of total collagen content. Briefly, 100 µL of the proteinase K-digested samples were hydrolyzed in 100 µL of 12 N hydrochloric acid at 110 $^{\circ}$C overnight and neutralized with 100 µL of 6 N sodium hydroxide. One hundred µL of dH$_2$O was added and the samples were centrifuged at 400 x g for 1 minute. The supernatant was analyzed as previously described[84]. Absorbance was read using a CLARIOstar® microplate reader at 560 nm. The hydroxyproline concentration was normalized to the dry weight of each sample.

Dimethylmethylene blue assay: The DMMB assay was used to quantify the sGAG content following decellularization in comparison to native tissue samples, as previously

reported[84]. Absorbance was read using a CLARIOstar® microplate reader at 525 nm. The sGAG concentration was normalized to the dry weight of each sample.

2.2.3   Immunohistochemical Staining

Native and decellularized intestine samples (n=3 cross-sections/batch, N=3 independent decellularization batches) were embedded in Tissue-Tek OCT compound (Sakura Finetek, CA, United States) and immediately placed on dry ice in preparation for cryosectioning, as described above. The sections were fixed in acetone for 10 minutes at -20°C and blocked in 10% goat serum in tris-buffered saline with 0.1% tween (TBST) for 1 hour at room temperature. The sections were then incubated overnight at 4°C with primary antibodies against collagen type I (dilution 1:100 in TBST with 2% BSA, ab34710, Abcam, ON, Canada), collagen type IV (dilution 1:100, ab6586, Abcam), fibronectin (dilution 1:150, ab23750, Abcam), and laminin (dilution 1:200, ab11575, Abcam). Next, an anti-rabbit secondary antibody conjugated to Alexa Fluor 594 (dilution 1:200, ab150080, Abcam) was added and the samples were incubated for 1 hour at room temperature. Samples were then mounted in fluoroshield mounting media with DAPI. All samples were prepared together and negative controls with the absence of primary antibodies were included for both native and decellularized samples. Images were acquired with an EVOS FL fluorescence microscope (Thermo Fisher Scientific Inc., ON, Canada).

2.3   Formation of Intestinal ECM and Composite Alginate-ECM Hydrogels

Figure 2.1 presents a schematic overview showing the process from tissue harvest to obtaining the pepsin-digested intestinal ECM that was used to generate hydrogels comprised exclusively of ECM (Aim 2) or incorporated within alginate to produce the composite alginate + ECM hydrogels (Aim 3).
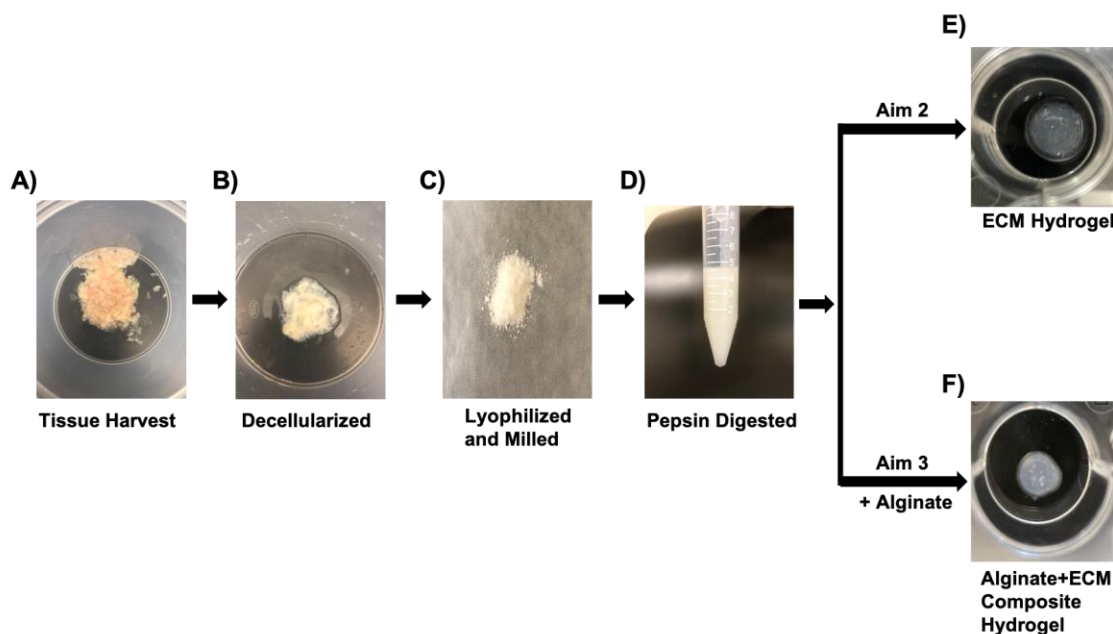
Figure 2.1 Process overview to generate the decellularized small intestinal ECM-derived hydrogels. A) Small intestine was isolated from multiple mice (N=35-40 mice) and pooled. The isolated intestines were **B)** decellularized using a novel protocol and then **C)** the decellularized small intestine ECM was freeze-dried and cryo-milled to generate a fine powder. **D)** The cryo-milled ECM was then digested with pepsin to generate an ECM solution that was used to fabricate the intestinal ECM-derived hydrogels. **E)** ECM-only derived hydrogel droplets, which were crosslinked through pH neutralization and incubation at 37 °C (50 μL in a 24-well plate). **F)** Composite hydrogels fabricated by combining the pepsin-digested ECM with alginate, which was crosslinked through incubation in a calcium chloride solution (50 μL droplet in 24-well plate).

2.3.1   Pepsin Digestion of Cryomilled Intestine

Lyophilized DSI samples were cryo-milled into a fine powder by placing each sample into a Retsch 25 mL grinding jar with two 10 mm stainless steel milling balls. The chambers were submerged in liquid nitrogen for 3 minutes prior to milling for 3 minutes at 30 Hz (Retsch Mixer Mill MM 400 milling system). This cycle was repeated for a total of three times. Cryomilled decellularized intestine were added at a concentration of 25 mg/mL to sterile 1 mg/mL porcine pepsin (3200-4500 mU/mg protein) (Sigma CAT#P6887) in 0.05 M hydrochloric acid (total volume 5 mL) and digested for 24 hours at room temperature under agitation at 100 rpm. Following digestion, while on ice, 1:10 volume of 10X PBS was added and the solutions were neutralized with 1 M sodium

hydroxide in 20 μL increments. The resultant solutions were stored at 4 °C and kept on ice during use.

2.3.2   Formation of Hydrogels Comprised Exclusively of ECM or Matrigel®

To generate the hydrogels comprised exclusively of intestinal ECM that were studied in Aim 2, the 25 mg/mL pepsin-digested DSI solution was combined in a 1:1 ratio with sterile filtered H_2O to obtain a final ECM concentration of 12.5 mg/mL. The diluted samples were pipetted in 50 μL droplets into a 24-well plate and crosslinked through incubation at 37 °C for 1 hour, to allow self-assembly of the collagen within the samples. Matrigel® hydrogels were similarly fabricated as a control, following the manufacturer's protocols.

2.3.3   Formation of Composite Alginate-Based Hydrogels

Composite alginate + DSI hydrogels were investigated in Aim 3 by combining the pepsin-digested DSI with alginate, which can be reversibly crosslinked through incubation in solutions containing divalent cations, such as calcium. Control hydrogels were fabricated from alginate alone, along with alginate combined with pepsin-digested decellularized meniscus (DM) (prepared and donated by Sheradan Doherty, Flynn lab), which was previously shown to induce the spreading of human adipose-derived stromal cells encapsulated within alginate gels. Alginate was prepared by dissolving alginic acid sodium salt, low viscosity (Alfa Aesar, B25266) in sterile filtered H_2O to obtain a 2% alginate concentration (w/v). The alginate solution was decontaminated for cell culture by heating it to 98 °C for 30 minutes and cooled at room temperature before use. Composite alginate-ECM gels were fabricated by combining 2% (w/v) alginate with pepsin-digested intestine, meniscus, or with sterile filtered H_2O in a 1:1 ratio. The samples were pipetted in 50 μL droplets into a 24-well plate and immersed in 2% (v/w) calcium chloride for 1 hour at 37 °C to crosslink the alginate, and then washed with PBS to remove excess calcium chloride.

2.4 *In vitro* Assessment of NIH 3T3 Cells Encapsulated in Hydrogels

2.4.1 NIH 3T3 Cell Culture and Encapsulation

A simplified cell culture model was used to validate that the pepsin-digested DSI generated with the novel decellularization protocol would have bioactive effects on cell populations encapsulated within the hydrogels, prior to moving on to the more complex and heterogeneous cell populations within the organoid cultures. For the studies in Aim 2, the viability, spreading and metabolic activity of NIH 3T3 cells encapsulated were assessed in the ECM-derived hydrogels comprised exclusively of pepsin-digested DSI in comparison to Matrigel® controls. Similar studies were performed in Aim 3, to compare the response of NIH 3T3 cells encapsulated in the alginate + DSI hydrogels, to alginate alone and alginate + DM hydrogel controls.

NIH 3T3 fibroblasts were cultured in proliferation medium comprised of DMEM (Wisent bioproducts, CAT# 319-005-CL) supplemented with 10% fetal bovine serum (Gibco®, Invitrogen, ON, Canada) and 1% penicillin/streptomycin (Gibco®, Invitrogen, ON, Canada) in a 5% CO_2 humidified incubator at 37 °C. To prepare the cells for the encapsulation studies, cryopreserved P3-P7 cells were thawed and plated on T-75 tissue culture polystyrene (TCPS) flasks (Corning, NY, United States) at a density of 5000 cells/cm^2 in DMEM and cultured at 37 °C (5% CO_2). The media was changed every 2 days, and cells were passaged at approximately 80% confluence. For passaging, the NIH 3T3 cells were released using trypsin-EDTA (0.25% Trypsin/2.21 mM EDTA from Wisent Inc., QC, Canada), centrifuged at 400 x g for 5 minutes, resuspended in media, and split into new T-75 flasks at a density of 5000 cells/cm^2.

For the cell encapsulation studies in Aim 2, the NIH 3T3 cells were combined with the diluted pepsin-digested DSI or Matrigel® at a concentration of 1.0 x 10^6 cells/mL and mixed well through gentle pipetting. The encapsulated gels were gently pipetted as 50 μL droplets onto 12-well cell culture inserts (Greiner Bio-one, Germany), and allowed to incubate at 37 °C (5% CO_2) for 1 hour before adding 3 mL of warm proliferation medium (1 mL in insert, 2 mL in well). Media was carefully changed every 2-3 days.

For the cell encapsulation studies in Aim 3, NIH 3T3 cells were combined with the alginate-based hydrogels (alginate + DSI, alginate + DM, alginate alone) at a concentration of 1.0 x 10^6 cells/mL and mixed well through gentle pipetting. The encapsulated gels were gently pipetted as 50 µL droplets onto 12-well cell culture inserts, which were subsequently immersed in 1 mL of 2% calcium chloride and incubated at 37 °C (5% CO_2) for 1 hour. Subsequently, the calcium chloride solution was removed, and the samples were rinsed with PBS, before adding 3 mL of warm proliferation medium (1 mL in insert, 2 mL in well). Media was carefully changed every 2-3 days.

2.4.2 Confocal Analysis of Cell Viability and Cell Spreading using the LIVE/DEAD® Assay

NIH 3T3 cell viability was assessed through confocal microscopy at 24 hours, 3 days, and 7 days post-encapsulation using the LIVE/DEAD® Viability/Cytotoxicity Assay (Invitrogen CAT#L3224). Live cells were identified through Calcein AM staining (green) and dead cells were labeled using ethidium homodimer-1 (EthD-1) (red). At each timepoint, triplicate gels (n=3 replicates/group at each timepoint, N=3 experimental repeats) from each group were rinsed with PBS and incubated at 37 °C in 4 µM EthD-1 and 2 µM Calcein AM in PBS for 45 minutes. Following incubation, non-overlapping images were taken using a 5X objective across the entire cross-section of each gel at defined depths ranging from 70 µm to 170 µm using the Zeiss LSM800 Confocal Microscope.

2.4.3 Metabolic Activity Analysis

The metabolic activity of the encapsulated 3T3 cells was assessed at 24 hours, 3 days, and 7 days post-encapsulation using the CyQUANT™ MTT Cell Viability Assay kit (Thermo Fisher Scientific Inc. CAT#V13154) (n=3 replicates/group, N=5 experimental repeats for Day 1 to Day 7 studies, N=3 for Day 7 only studies), following previously published methods[116]. In brief, the samples were incubated in 3 mL (1 mL in insert, 2 mL in well) of MTT solution (0.5 mg/mL in cell culture medium) at 37 °C for 4 h. Next, each sample was crushed within a microcentrifuge tube using a plastic pestle, and subsequently incubated in 800 µL of DMSO for 1 h at 37 °C under agitation (100 rpm) to

extract the formazan crystals. Samples were then centrifuged at 15,000 x g for 15 minutes to remove the gels and only the supernatant was used for measurements. The absorbance was measured at 540 nm and corrected for background absorbance at 690 nm using a CLARIOstar® Multimode Microplate Reader (BMG Labtech, ON). In addition, the absorbance values from unseeded hydrogel controls were subtracted from the values for the hydrogels containing the encapsulated 3T3 cells to account for potential background associated with the presence of scaffolding materials.

2.5   Intestinal Organoid Culture

2.5.1   Isolation of Intestinal Crypts

After confirming that the pepsin-digested DSI had bioactive effects on NIH 3T3 cells, the next studies focused on encapsulating primary intestinal organoids within the hydrogels to evaluate the ability of pepsin-digested DSI to support intestinal organoid growth and viability. For the studies in Aim 2, the growth of intestinal organoids over 14 days was assessed in the ECM-derived hydrogels comprised exclusively of pepsin-digested DSI in comparison to Matrigel® controls. Similar studies were performed in Aim 3, to compare the response of intestinal organoids encapsulated in the alginate + DSI hydrogels to alginate alone.

Adult male and female C57BL/6 mice (2–4 months in age) were euthanized by CO_2 overdose and their small intestines were surgically extracted. The methods for organoid culture were adapted from methods previously described by Sato *et al*[36]. Briefly, the small intestines were perfused with PBS using a needle and syringe to remove intestinal contents. Next, the intestines were cut open longitudinally and scraped using a glass cover slip to remove the villi. The intestines were then cut into 0.5 mm pieces and transferred into a 50 mL centrifuge tube and washed vigorously with PBS 3-5 times. Following PBS washing, the intestinal tissue was resuspended in 10 mL of 2.5 mM EDTA in PBS and incubated at 4 °C in a rotator for 45 minutes. The PBS solution was then removed, and the intestine was resuspended in 10 mL of fresh PBS. Once resuspended, the solution was pipetted 10-15 times to release the crypts from the tissue fragments. The solution was then passed through a 70 µM cell strainer and centrifuged at

88 x g for 5 minutes. The pellet was resuspended in 5 mL DMEM (Fisher) containing 1X Glutamax (Life Tech), 1X (4-(2-hydroxyethyl)-1-piperazineethanesulfonic acid) (Hepes; LifeTech), and 1X antibiotic/mycotic penicillin and streptomycin solution (Life Tech). The samples were then centrifuged at 50 x g for 5 minutes and the supernatant was removed. The pellet of crypts was counted, and the crypts were then resuspended in the appropriate volume of Matrigel® (Fisher CAT#356231) to obtain ~2000 intestinal crypts/mL. Twenty-four well plates were pre-warmed in the incubator prior to adding 50 µL droplets of Matrigel® per well. Plates were warmed in the incubator for 10 minutes prior to adding 500 µL of DMEM. Each well was supplemented with 50 ng/mL epidermal growth factor (EGF), 1 µg/mL R-spondin, and 100 ng/mL mNoggin. Media was changed every 4 days, and with fresh supplements added every other day.

2.5.2   Organoid Passaging and Encapsulation

Intestinal organoids were first cultured and maintained in Matrigel® before passaging into the hydrogels fabricated in Aim 2 and Aim 3. Intestinal organoids were passaged every 8-12 days. Briefly, media was removed from each well and replaced with 1 mL of cold DMEM to disrupt the Matrigel®. The organoids were pipetted up and down using a 1000 µL pipette tip to release them from the Matrigel® and transferred into a 15 mL tube. The organoids were then broken into smaller fragments by pipetting up and down with a glass Pasteur pipet 5-10 times and then centrifuged for 5 minutes at 50 x g before being resuspended and re-seeded in either the pepsin-digested DSI hydrogels or Matrigel® (Aim 2), or the alginate-based hydrogels (alginate + DSI, alginate + DM, alginate alone) (Aim 3), following the methods described above. Furthermore, to assess the viability of intestinal stem cells in the DSI hydrogels (Aim 2), the organoids grown for 14 days in DSI hydrogels were passaged back into fresh DSI or Matrigel®.

2.5.3   Organoid Imaging and Area Analysis

Organoids in both Aim 2 and Aim 3 were imaged at days 1, 7, and 14 which were an early, intermediate, and late timepoint, respectively, using 4x-20x objectives on the EVOS FL Auto. Two-dimensional image analysis was performed to measure the change

in organoid area from day 1 to day 7 post-encapsulation in either the pepsin-digested DSI hydrogels and Matrigel® (Aim 2), or in the alginate-based hydrogels (alginate + DSI and alginate alone) (Aim 3). Non-overlapping images were taken at a constant depth of each gel using a 4X objective. The same gels and regions were imaged on both days 1 and day 7. Organoid area was measured using the ImageJ software. For organoid area quantification, the area of n > 100 organoids per group was quantified/timepoint using positive pixel counting, and used to estimate the average fold-change in size from days 1 to 7 as a measure of organoid growth.

2.5.4   Histological Analysis

Intestinal organoids cultured for 10 days in either Matrigel® or DSI hydrogels (Aim 2) were fixed overnight at 4 °C in 4% paraformaldehyde. Next, the paraformaldehyde was removed, and the samples were carefully rinsed with PBS. Two hundred μL of pre-warmed 2% (v/w) agarose was carefully added to the wells and allowed to solidify at room temperature. The agarose gels containing the encapsulated organoids were then carefully embedded in Tissue-Tek OCT compound and immediately placed on dry ice in preparation for cryosectioning (7 μm sections) with a Leica CM3050 S cryostat. Samples were warmed at room temperature for 15 minutes and then rinsed in H_2O. Sections were stained with hematoxylin and eosin to visualize the cells within the surrounding ECM following standard protocols. Eosin (eosinophilic) which is an acidic dye is negatively charged and stains basic structures like cytoplasm and extracellular proteins red or pink. Hematoxylin (basophilic), on the other hand, is a basic dye that stains acidic structures such as the nuclei in a purplish blue color. Images were obtained using the EVOS FL Auto.

2.6   Statistical Analyses

All statistical analysis were performed using GraphPad Prism 7.0. Statistical analyses were carried out by t-test and two-way ANOVA as detailed in the figure captions. Three normality tests were carried out for all studies, however due to low statistical power (low N value), tests either passed for normality or did not have a large enough sample size. All

numerical data are expressed as mean ± standard deviation (S.D.). Differences with $p < 0.05$ were considered statistically significant.

Chapter 3

3 Results

3.1 Characterization of Decellularized Intestinal Tissues

The first aim of this project was to establish a novel mouse intestinal decellularization protocol that removes cellular content while preserving the extracellular matrix (ECM) composition. The small intestine from 35-40 adult mice was processed together as a single batch of decellularized tissue. Briefly, the novel decellularization protocol developed involved dissecting the small intestine from adult mice, followed by mincing and processing the tissue using a 4-day process that included freeze-thaw cycles in hypotonic solutions, Triton X-100 detergent extractions, and enzymatic digestion using deoxyribonuclease (DNase) and ribonuclease (RNase).

Decellularized samples were compared to native tissue controls using histological and biochemical analyses. To assess the removal of cellular components, hematoxylin and eosin (H&E) staining was performed, which stains cellular components in purple and ECM components in pink (Figure 3.1). Representative H&E staining of the native and decellularized small intestine (DSI) showed that the protocol effectively removed cellular components (absence of purple stained nuclei on the right panel of Figure 3.1), while retaining ECM components, with only the pink staining characteristic of collagen visualized in the DSI samples.
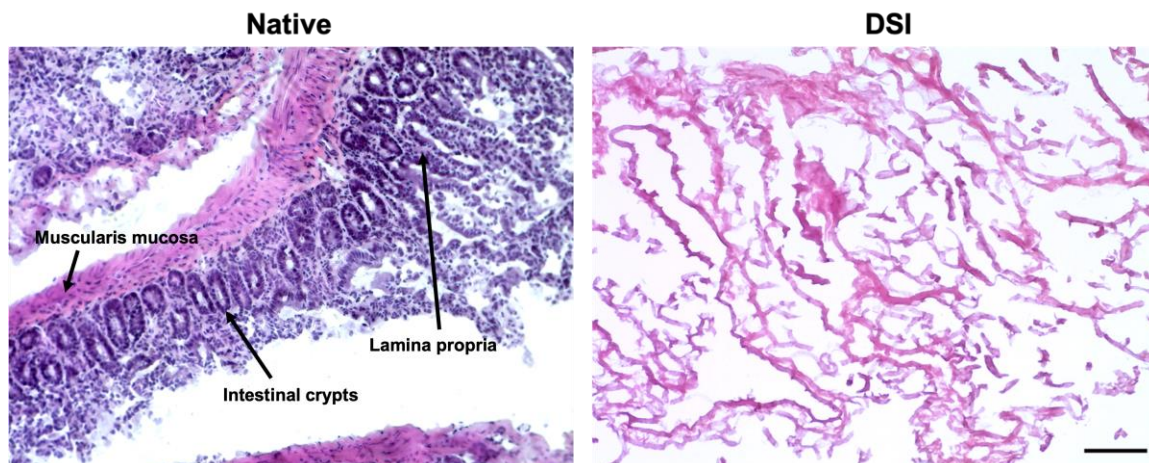
Figure 3.1. H&E staining confirms effective removal of cellular content following decellularization. Representative H&E staining of native and DSI showing effective removal of cellular components (including absence of basophilic cell nuclei that normally stain purple) while retaining ECM components (stained pink due to its eosinophilic nature and staining is characteristic of collagen) following decellularization. Black arrows indicate specific intestinal regions including muscularis mucosa, intestinal crypts, and lamina propria (n=3 cross-sections/decellularization batch, N=3 independent decellularization batches). Scale bar=100 μm.

To confirm the effectiveness of cell extraction, 4',6-diamidino-2-phenylindole (DAPI) fluorescence staining was performed to visualize cell nuclei within the DSI samples relative to native tissue controls (Figure 3.2A). Notably, no visible nuclei remained in the tissues at the end of processing. To further validate these findings, the PicoGreen assay was used to quantify the double-stranded DNA (dsDNA) content in the native and DSI samples (Figure 3.2B). A significant reduction in the dsDNA content was observed following decellularization, with an average decrease of $91.56 \pm 9.73\%$ relative to native tissue controls.

A) Native   DSI

B)
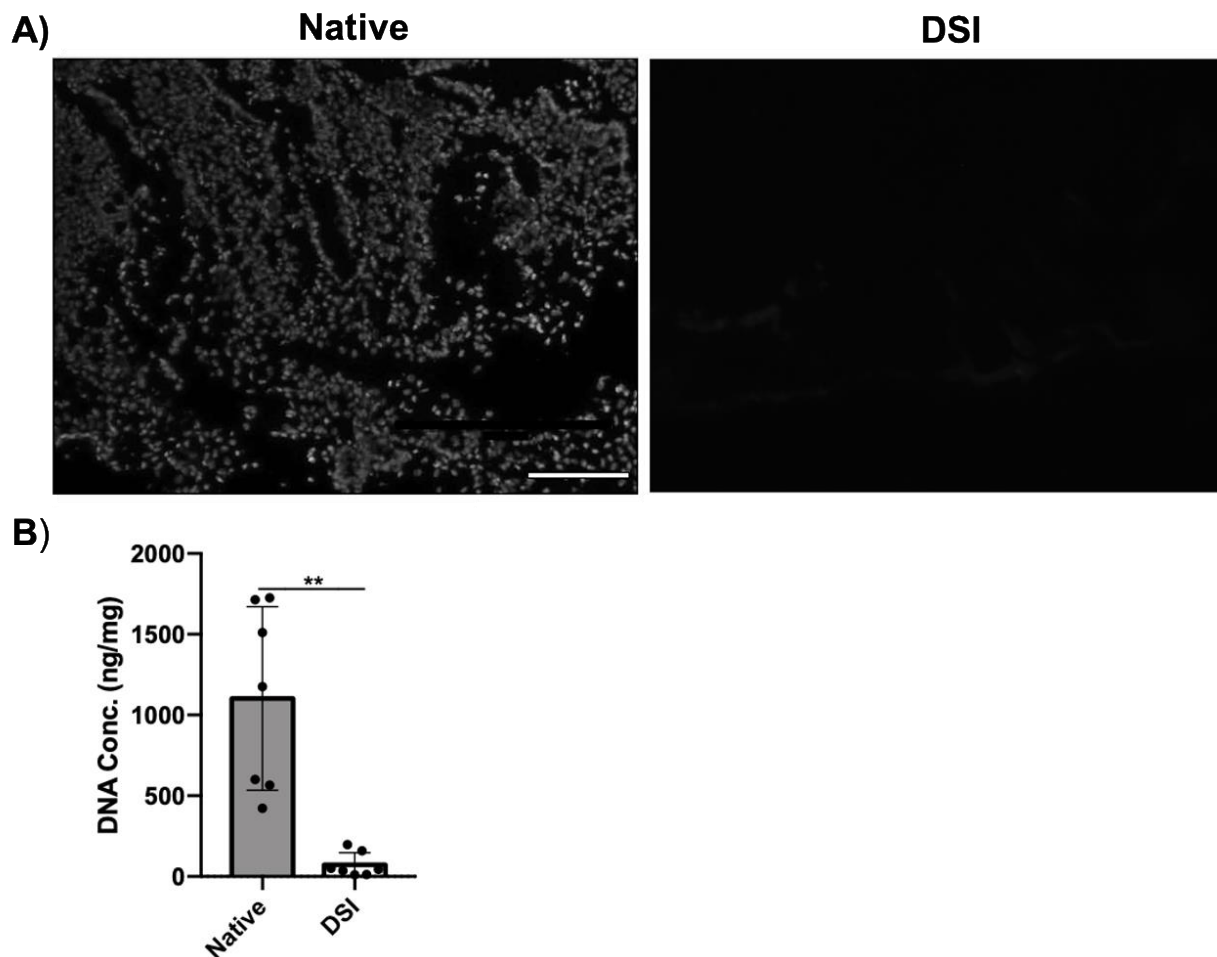
Figure 3.2. DAPI staining and PicoGreen quantification verify that the new decellularization protocol effectively extracted cellular contents from the mouse small intestines. A) Representative DAPI nuclear staining (shown in grayscale) of native (left panel) versus DSI (right panel) mouse small intestine, with no visible nuclei detected following decellularization (n=3 cross-sections/decellularization batch N=3 independent decellularization batches). Scale bar=100 μm. **B)** Quantitative analysis of double-stranded DNA (dsDNA) content using the PicoGreen assay confirmed that decellularization was effective at extracting cells from the tissues. Values are reported based on dry weight. (N=7 independent decellularization batches). Mean ± S.D, Paired *t*-test; **p<0.01.

Following decellularization, the collagen content of the intestinal tissue samples was assessed. The samples were stained using picrosirius red and imaged using polarized light microscopy to visualize the network of collagen fibers. The imaging revealed a qualitatively denser network of collagen fibers stained red in the DSI tissues relative to the native tissue controls (Figure 3.3A). In addition, a hydroxyproline assay was used to

quantify the collagen content in the native tissue and DSI samples (Figure 3.3B), revealing a significant increase in the relative collagen content following decellularization, consistent with the removal of cells and potentially other ECM constituents.
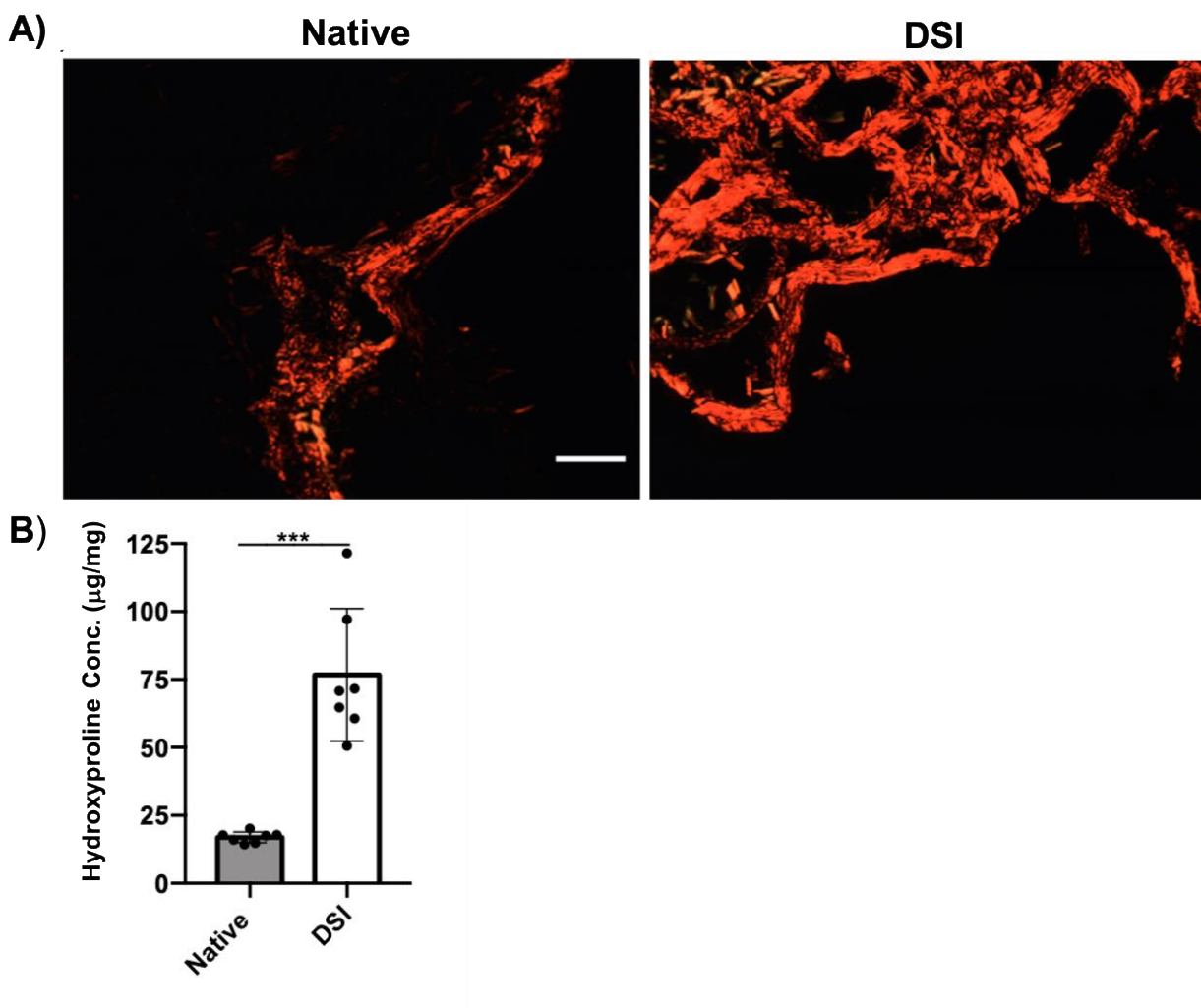
Figure 3.3. Picrosirius red staining and the hydroxyproline assay indicate an increase in the relative collagen content following decellularization. A) Representative images of picrosirius red staining showing that the DSI contained a qualitatively more dense network of collagen fibers than the native tissue samples. (n=3 cross-sections/decellularization batch, N=3 independent decellularization batches). Scale bar=500 μm. **B)** Quantification of total collagen content by the hydroxyproline assay showed higher relative levels in the DSI samples relative to the native tissue controls. Values are reported based on dry weight. (N=7 independent decellularization batches). Mean ± S.D, Paired t-test; ***p<0.001.

Glycosaminoglycan (GAG) content was assessed by toluidine blue staining and the dimethylmethylene blue assay (Figure 3.4). Toluidine blue staining revealed qualitatively similar levels of GAG staining (purple) in the DSI samples compared to the native tissues (Figure 3.4A). Moreover, the DMMB assay confirmed there were similar levels of sulphated GAGs (sGAG) in both the DSI and native small intestine samples, with no significant difference observed between the groups.
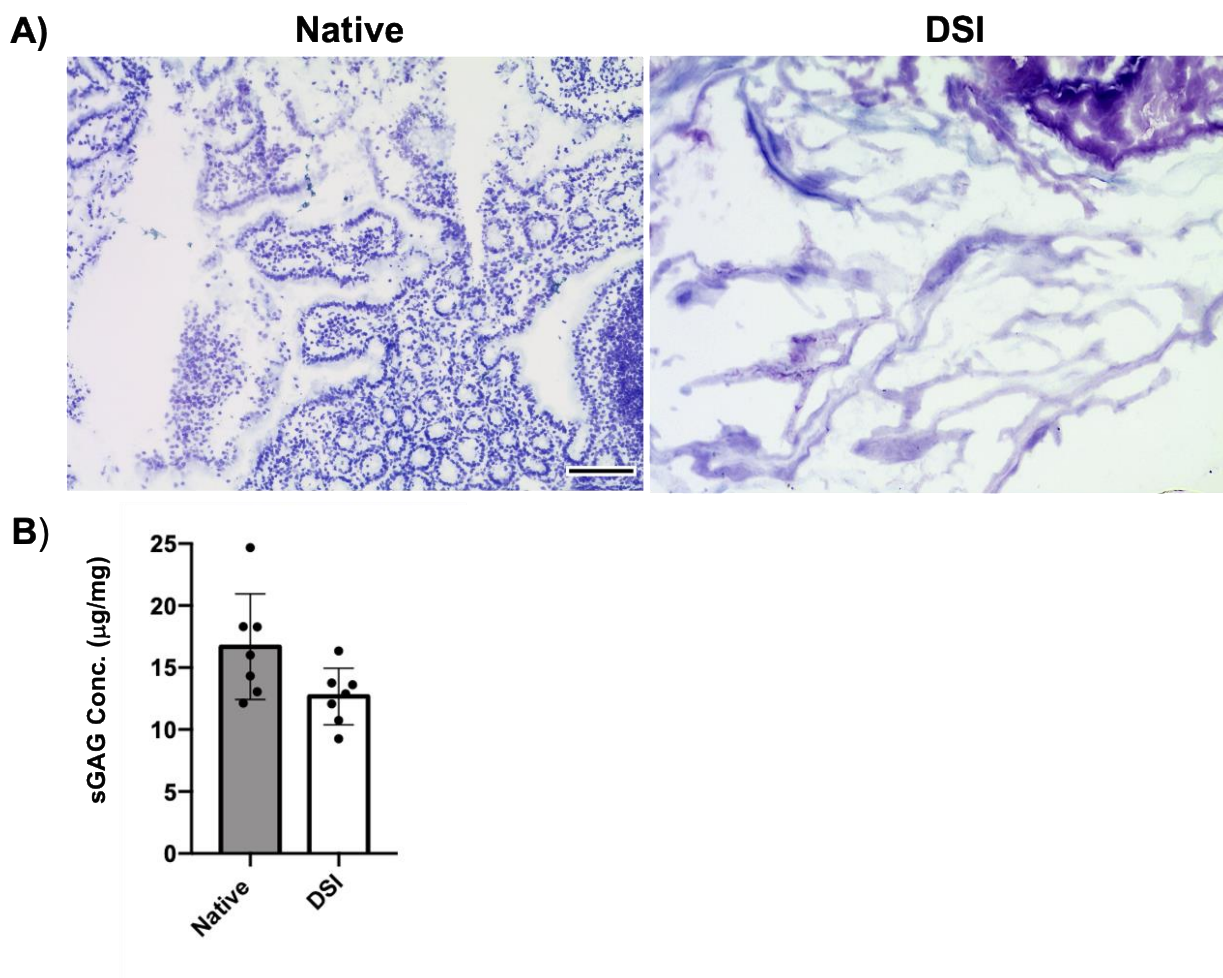
Figure 3.4. Sulphated glycosaminoglycan (sGAG) content was retained following decellularization. A) Representative toluidine blue staining showing staining of GAGs (purple) and nucleic acids (blue) in the native versus DSI. (n=3 cross-sections/decellularization batch, N=3 independent decellularization batches). Scale bar=100 μm. **B)** Quantitative analysis of sGAG content with the DMMB assay showed similar levels in the native and DSI samples. Values are reported based on dry weight. (N=7 independent decellularization batches). Mean ± S.D, Paired *t*-test.

Immunohistochemical staining was additionally used to confirm the presence of key ECM components in the DSI samples, and compare their distribution relative to the native tissue controls (Figure 3.5). Immunofluorescence staining confirmed the retention of collagen I, collagen IV, fibronectin, and laminin following decellularization, which were all well distributed throughout both the DSI and native tissue samples.
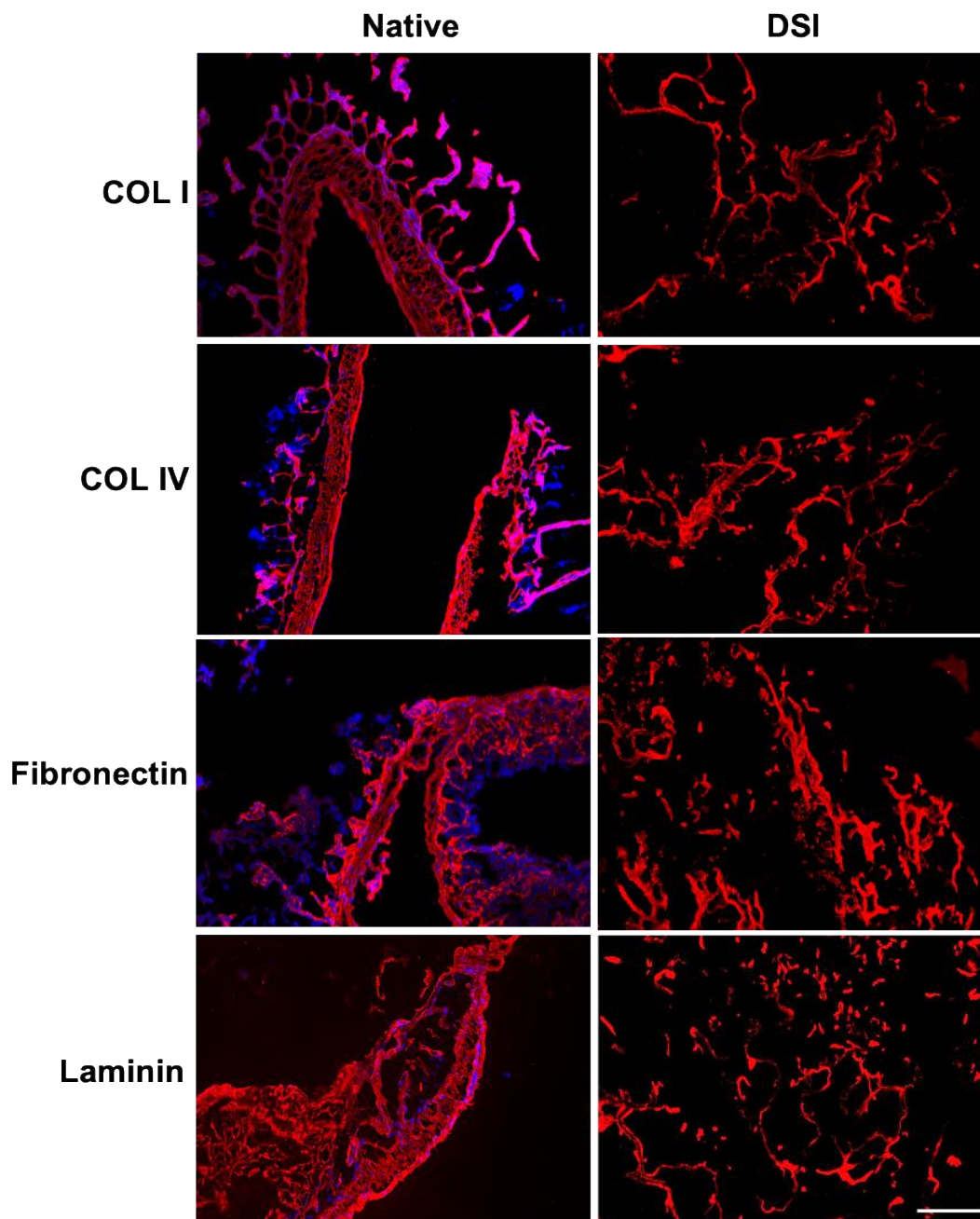
Figure 3.5. Immunofluorescence staining confirmed the retention of ECM components following decellularization. Representative staining for collagen I, collagen IV, fibronectin, and laminin following decellularization demonstrated retention of all markers of interest. All samples were counterstained with DAPI (blue) for cell nuclei. (n=3 cross-sections/decellularization batch, N=3 independent decellularization batches). Scale bar=200 μm. Abbreviations: COL I=collagen type I, COL IV=collagen type IV.

3.2 *In Vitro* Assessment of NIH 3T3 Cells Encapsulated and Cultured in Intestinal ECM Hydrogels and Matrigel®

DSI generated in Aim 1 was lyophilized, cryo-milled, and enzymatically digested with pepsin. The pepsin-digested ECM, with a final ECM concentration of 12.5 mg/mL, was incubated at 37 °C for 1 hour to create the hydrogels. To confirm the bioactivity of the ECM generated with the novel decellularization protocols, a LIVE/DEAD assay was used with confocal imaging to assess cell viability and spreading of NIH 3T3 murine fibroblasts encapsulated within the DSI hydrogels, relative to Matrigel® controls at days 1, 3, and 7 post-encapsulation (Figure 3.6A). Both groups showed qualitatively similar viability and cell spreading, an indication of cell attachment to ECM components, over the 7-day culture period, with the staining patterns indicating that the cells were proliferating over time.

To verify these results, the MTT assay was performed to quantitatively compare the metabolic activity of the encapsulated 3T3 cells within the DSI hydrogels and Matrigel® controls (Figure 3.6B). There were no significant differences in the metabolic activity between the groups at any of the time points examined. Further, there was a significant increase in metabolic activity on day 7 as compared to days 1 and 3 for both groups, consistent with an increase in cell number.

To additionally assess batch-to-batch variability in the decellularization process (i.e. ECM derived from tissues processed separately), the metabolic activity of the encapsulated NIH 3T3 cells was assessed on day 7 in DSI hydrogels prepared from three independent decellularization batches relative to Matrigel® controls (Figure 3.6C). Importantly, minimal variation was observed between the 3 ECM batches, supporting that the protocol was robust and repeatable for generating bioactive ECM that could support the viability and growth of encapsulated cell populations.
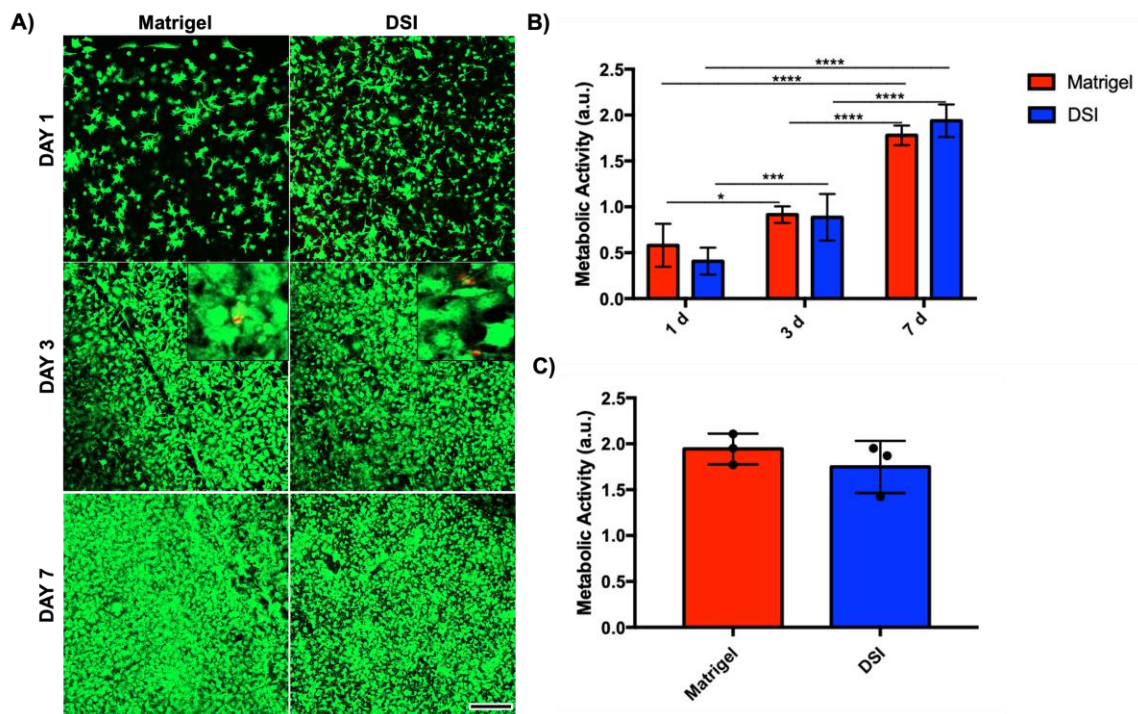
Figure 3.6. Assessment of cell viability and metabolic activity of NIH 3T3 murine fibroblasts encapsulated within DSI hydrogels or Matrigel® controls showed that both platforms similarly supported cell viability and growth. A) Representative confocal microscopy images showing stained calcein$^+$ live (green) and EthD-1+ dead (red) 3T3 fibroblasts within DSI hydrogels or Matrigel® controls. High cell viability was maintained with both platforms over the 7-day culture period. Cell spreading was observed at all time points in both groups. Insets on Day 3 show the presence of infrequent red (dead) cells. (n=3 hydrogels per timepoint/trial, N=3 trials with independent ECM batches). Scale bar=500 µm. **B)** Quantification of metabolic activity using a MTT assay showed similar metabolic activity in 3T3 cells encapsulated within the DSI hydrogels or Matrigel® across all time points. Higher metabolic activity levels were observed at day 7 as compared to day 1 and 3 for both groups, consistent with cell proliferation. (N=5 separate 3T3 encapsulations). Mean ± S.D, Two-way ANOVA; *p<0.05, ***p<0.001, ****p<0.0001. **C)** Metabolic activity of 3T3 cells encapsulated in DSI hydrogels prepared from different ECM batches, showing consistency in the response to the developed bioscaffolds and comparable metabolic activity levels to Matrigel® controls at 7 days post-encapsulation. (N=3 independent decellularized and pepsin-digested DSI batches). Mean ± S.D, Unpaired *t*-test. Metabolic activity was measured by absorbance values in arbitrary units (a.u.) (**B-C**).

3.3 *In Vitro* Assessment of Mouse Intestinal Cells Encapsulated and Cultured in Intestinal ECM Hydrogels and Matrigel®

To assess the ability of DSI hydrogels to promote intestinal organoid growth, primary mouse intestinal organoids were first cultured in Matrigel® prior to being passaged and encapsulated within both Matrigel® and DSI hydrogels (Figure 3.7). Intestinal organoids were cultured for 14 days and imaged on days 1, 7, and 14 post-encapsulation (Figure 3.7A). Organoid growth over 14 days appeared qualitatively similar in the DSI hydrogels as compared to Matrigel®. Images taken at higher power on day 7 post-encapsulation revealed budding in the organoids and granule-containing cells in the budding crypts of both Matrigel®- and DSI-grown organoids (Figure 3.7B). Organoid area was calculated using Image J on day 1 and 7 post-encapsulation. The fold change in organoid area on day 7 relative to day 1 was similar in the DSI hydrogels and Matrigel® controls (Figure 3.7C). Representative H&E staining of different organoids grown in Matrigel® or DSI at 10 days post-encapsulation show an epithelial layer (purple stained nuclei) with budding crypts surrounding a hollow lumen (Figure 3.7D).
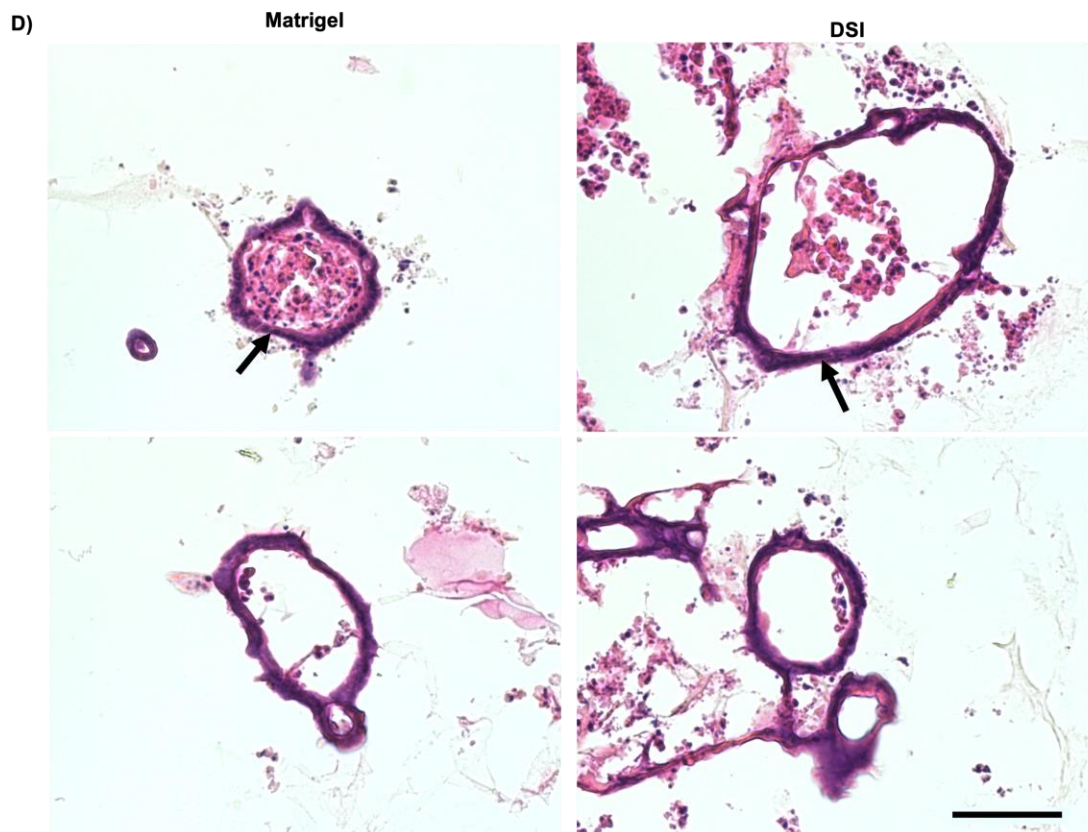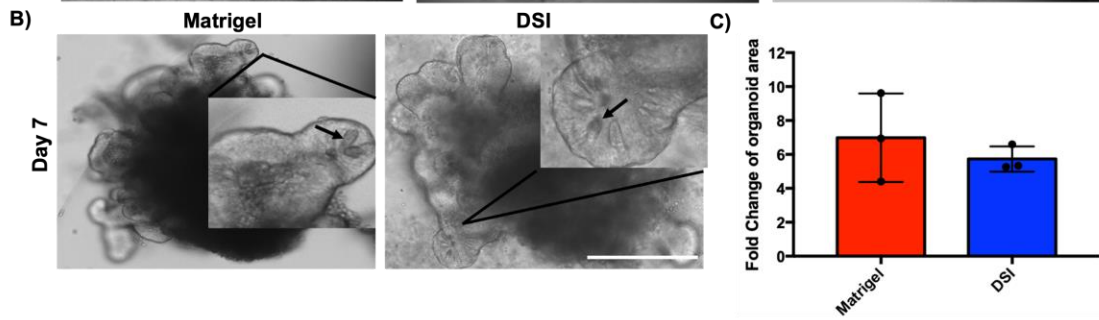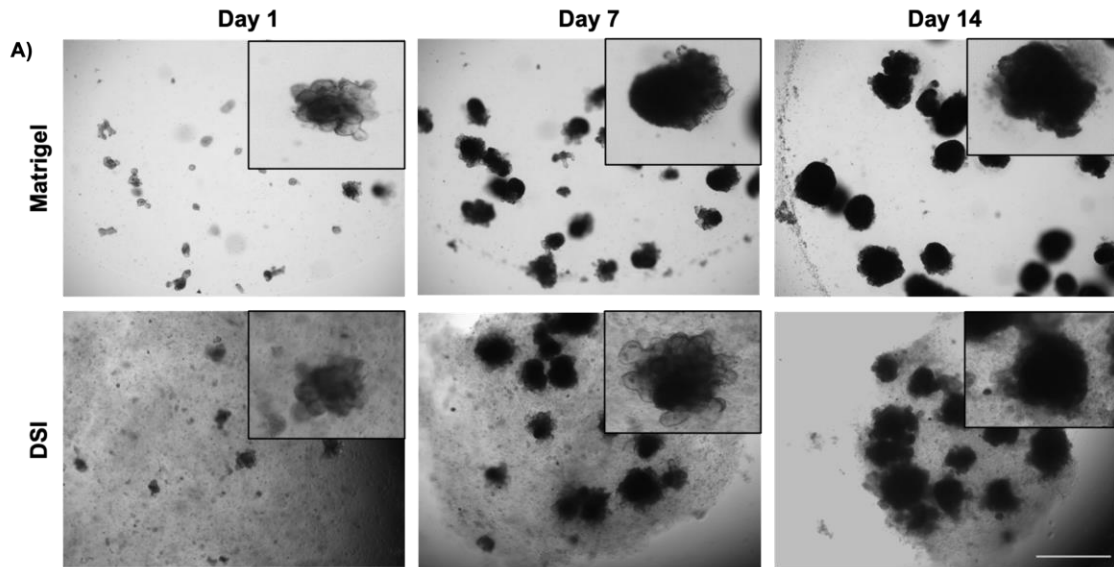
Figure 3.7. DSI hydrogels promote the growth of mouse intestinal organoids *in vitro*.
A) Time course of mouse intestinal organoid growth is shown. Comparable organoid growth was seen over a 14-day culture period in the DSI hydrogels as compared to Matrigel® controls. Insets show high power images of a single organoid over the culture period. (N=3 independent ECM batches). Scale bar=1 mm. **B)** Representative brightfield microscopy images of organoids grown in Matrigel® versus DSI hydrogels at day 7. Images of organoids encapsulated within both Matrigel® and DSI hydrogels revealed granule-containing cells in the budding crypts, consistent with the presence of Paneth cells (black arrows). Scale bar=200 μm. **C)** Quantification of size of organoids grown in Matrigel® versus DSI hydrogels from day 1 to 7, showing similar organoid growth in both groups. (n ≈ 175 organoids per group were quantified/timepoint, N=3 independent organoid cultures). Mean ± S.D, Unpaired *t*-test. **D)** Representative H&E staining of different organoids grown in Matrigel® versus DSI hydrogels at day 10 post-encapsulation. Images revealed an epithelial monolayer (black arrows) surrounding a lumen in both hydrogels. (n=3 cross-sections, N=3 independent organoid cultures). Scale bar 50=μm.

Next, mouse intestinal organoids grown in DSI hydrogels were passaged into either Matrigel® or DSI hydrogels and imaged on days 1, 7, and 14 to assess growth as an indicator of viability (Figure 3.8A). The organoids encapsulated within the DSI hydrogels and Matrigel® both showed growth over the 14 day culture period. However, there were fewer organoids that increased in size in the DSI hydrogels as compared to Matrigel® (Figure 3.8B).
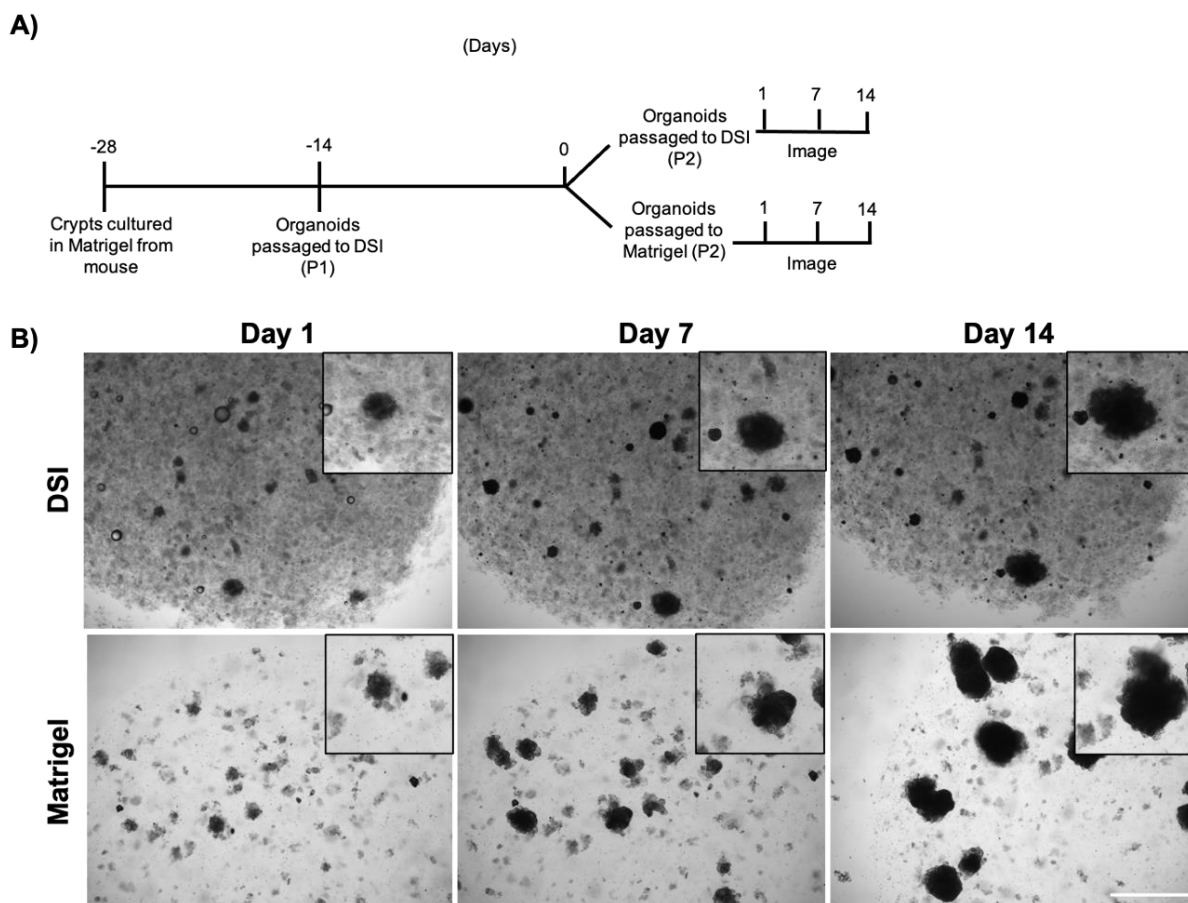
Figure 3.8. Organoids remain viable following passaging from the DSI hydrogels. A) Schematic of the timeline for organoid culture followed in panel B. **B)** Representative brightfield microscopy images of mouse intestinal organoids cultured in DSI hydrogels and then passaged into new DSI hydrogels or Matrigel®. Images were taken at days 1, 7, and 14 post-passaging. Intestinal organoids passaged into either DSI hydrogels or Matrigel® were followed over 14 days, with fewer growing organoids in the DSI hydrogel group versus the Matrigel® controls. (N=3 independent ECM batches). Scale bar=1 mm.

3.4 *In Vitro* Assessment of NIH 3T3 Cells Encapsulated and Cultured in Alginate-based Hydrogels

DSI generated in Aim 1 was incorporated within alginate to form a composite hydrogel platform, which may have more tunable mechanical properties and allow for reversible cell encapsulation. Three groups were investigated: 1% alginate, 1% alginate + DSI, and 1% alginate + Decellularized Meniscus (DM), as a positive control for cell spreading. The alginate-based hydrogels were crosslinked using calcium chloride for 1 hour at 37 °C.

Similar to the previous studies with the hydrogels comprised exclusively of DSI, initial testing focused on confirming that the ECM had bioactive effects within the composites using encapsulated 3T3 murine fibroblasts. The LIVE/DEAD assay with confocal imaging confirmed that all groups showed high viability across the 7-day culture period (Figure 3.9A). Cell spreading was observed in the alginate + DSI and alginate + DM groups, whereas the alginate alone group had a spherical cell morphology, supporting that the incorporated ECM provided cell-adhesive cues. The MTT assay showed that the metabolic activity was higher in the fibroblasts encapsulated within the alginate + DSI hydrogels compared to the cells encapsulated in alginate alone, and similar to alginate + DM control group at days 1, 3, and 7 post encapsulation (Figure 3.9B). The metabolic activity of cells encapsulated within the alginate + DSI hydrogels was higher at day 7 relative to day 1 and day 3, consistent with cell growth in the composites but not the alginate alone controls. Assessment of batch-to-batch variability using the MTT assay at day 7 post-encapsulation, showed consistent results in the composite hydrogels generated with 3 different DSI batches (Figure 3.9C).

A)
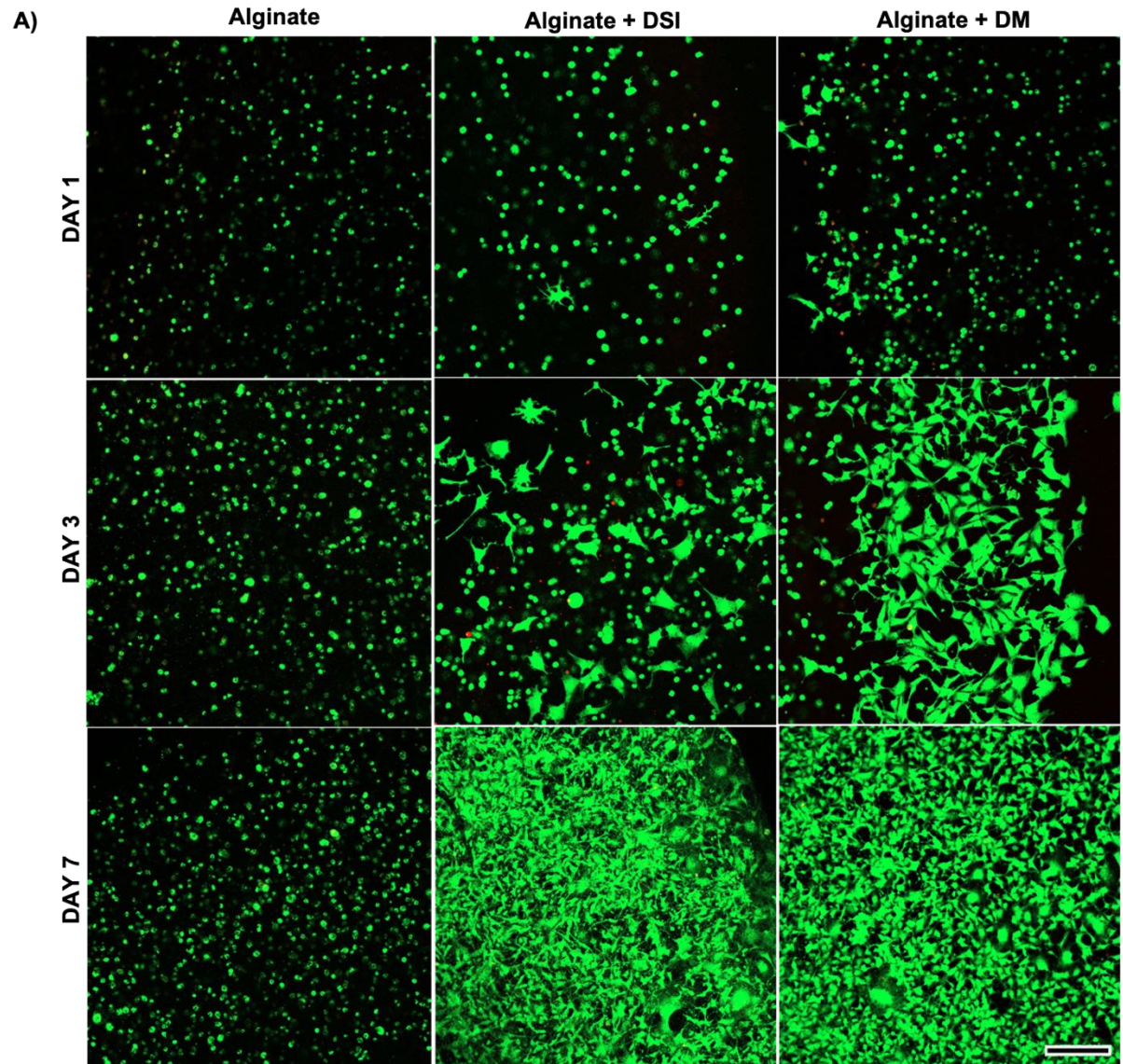
B)
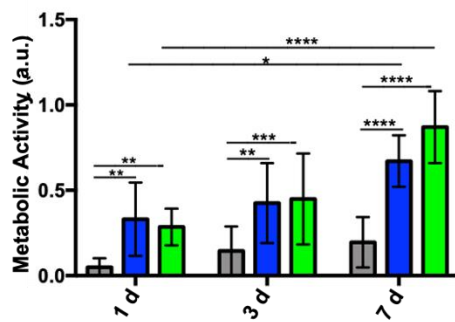
C)
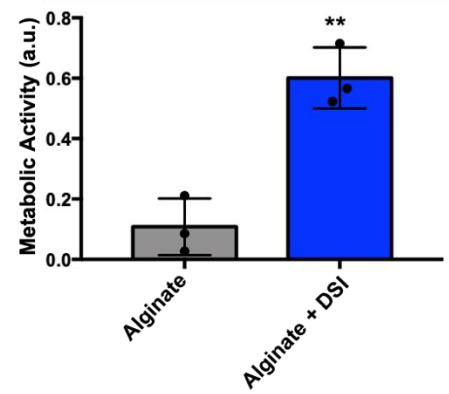
Figure 3.9. Incorporation of pepsin-digested DSI within alginate hydrogels promoted cell spreading and growth of encapsulated NIH 3T3 murine fibroblasts. **A)** Representative confocal images showing calcein$^+$ live (green) and EthD-1+ dead (red) 3T3 fibroblasts in all hydrogels, supporting that high cell viability was maintained throughout the culture period. Cell spreading was observed at all time points in the alginate + DSI and alginate + DM hydrogels, but not in the alginate alone control group. (n=3 hydrogels per timepoint/trial, N=3 trials with independent ECM batches). Scale bar=500 μm. **B)** Quantification of metabolic activity through the MTT assay showed higher metabolic activity levels in the alginate + DSI group relative to the alginate alone at all time points, supporting that the incorporated ECM had bioactive effects on the encapsulated cells. Metabolic activity levels of the cells encapsulated within the alginate + DSI hydrogels was higher at 7 days as compared to both day 1 and day 3, consistent with cell proliferation when the ECM was incorporated. (N=5 separate 3T3 encapsulations). Mean ± S.D, Two-way ANOVA; *$p<0.05$, **$p<0.01$, ***$p<0.001$, ****$p<0.0001$. **C)** Quantification of metabolic activity through the MTT assay showed consistently higher levels of metabolic activity at 7 d in the alginate + DSI samples relative to the alginate alone across three separate ECM batches. (N=3 independent decellularized and pepsin digested ECM batches). Mean ± S.D, Unpaired *t*-test. Metabolic activity was measured by absorbance values in arbitrary units (a.u.) (**B-C**).

3.5 *In Vitro* Assessment of Intestinal Organoids Encapsulated within Alginate-based Hydrogels

To assess the ability of alginate-based hydrogels to support the growth of intestinal organoids, primary mouse intestinal organoids were cultured in Matrigel® prior to being passaged and encapsulated within alginate alone or composite alginate + DSI hydrogels (Figure 3.10). Intestinal organoids were imaged using brightfield microscopy on days 1, 7, and 14 post-encapsulation (Figure 3.10A). Organoids seemed visibly similar in the alginate + DSI hydrogels versus the alginate alone hydrogels. More specifically, there was no noticeable change in the size or structure of the organoids in the alginate + DSI hydrogels on day 14 as compared to days 1 and 3. To verify the lack of apparent organoid growth, the organoid area was calculated on day 1 and 7 post-encapsulation using ImageJ (Figure 3.10B). The fold change in organoid area was similar in the alginate + DSI hydrogels as compared to the alginate alone group, with neither group showing a significant increase in size over time.
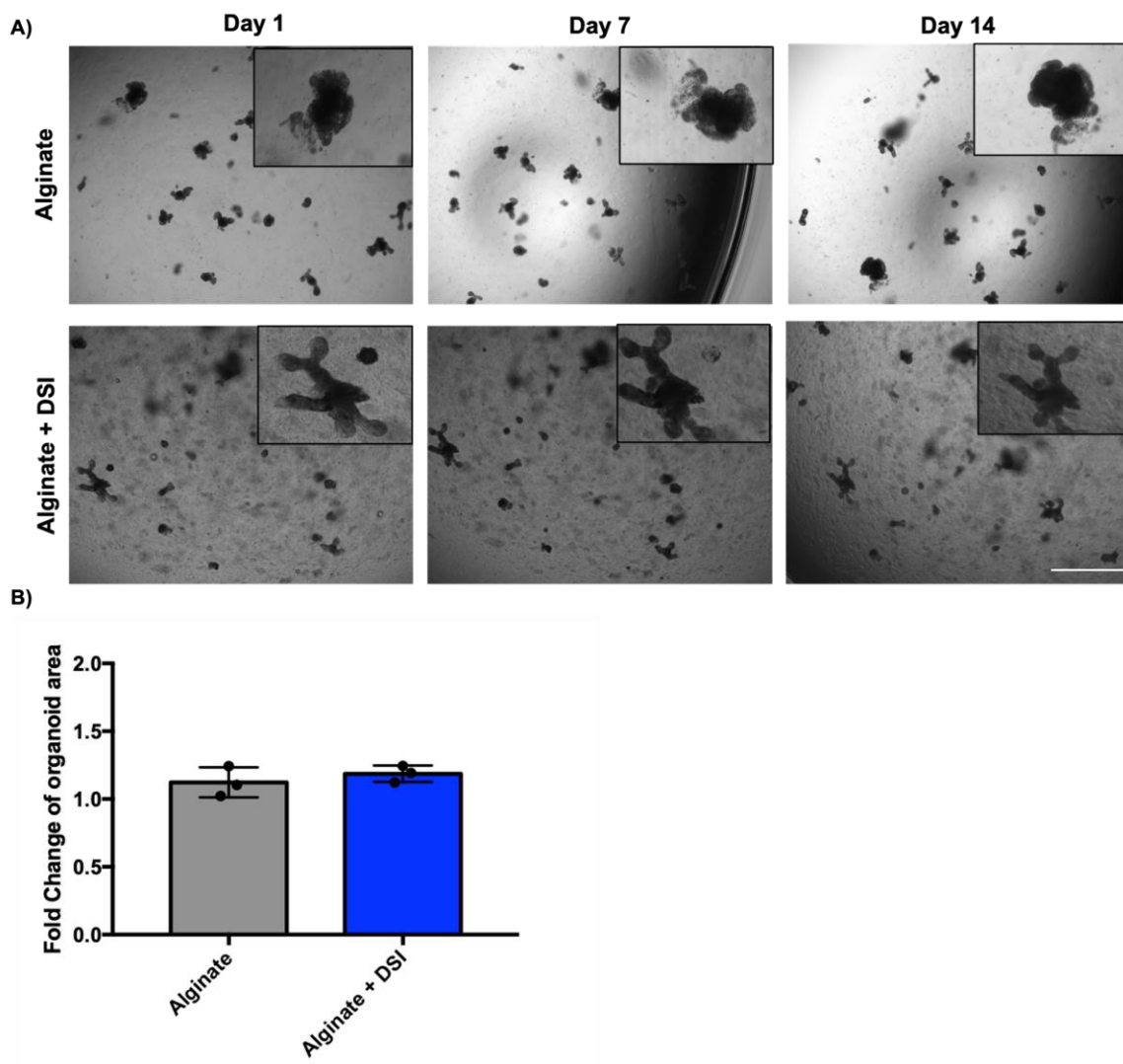
Figure 3.10. The incorporation of DSI within the alginate hydrogels was insufficient to promote the growth of mouse intestinal organoids *in vitro*. A) Time course of mouse intestinal organoids showed a lack of organoid growth over 14 days in both the alginate + DSI group and alginate alone group. (N=3 independent ECM batches). Scale bar=1 mm. **B)** Analysis of the change in size of organoids cultured in alginate versus alginate + DSI from days 1 to 7 post-encapsulation. The analysis showed no organoid growth in both hydrogels. (n ≈ 100 organoids per group/timepoint, N=3 independent organoid cultures). Mean ± S.D, Unpaired *t*-test.

Chapter 4

4   Discussion

The primary objective of this thesis was to develop a tissue-specific extracellular matrix (ECM)-derived bioscaffold that could replace Matrigel® in intestinal stem cell (ISC)-based organoid cultures. Matrigel® is an ECM product produced by mouse sarcoma cells that is enriched in basement membrane components. While it provides a highly supportive microenvironment for organoid growth[36,48–50] the fact that Matrigel® is derived from a cancer cell line limits its clinical applicability[51,52]. As an alternative, bioscaffolds derived from decellularized tissues can mimic the native ECM and provide tissue-specific biological cues that can regulate proliferation and differentiation[64]. In this study, a novel decellularization protocol was developed for isolating the small intestinal ECM from mouse tissues and methods were established to generate hydrogels incorporating the decellularized small intestine (DSI) that could be used to encapsulate and culture intestinal cells.

In contrast to many protocols in the literature[56,67,74,81,85,88,89], the decellularization protocol developed avoids the use of stronger ionic detergents, which can cause greater loss of more soluble ECM components including growth factors and glycosaminoglycans (GAGs)[67,117], and can be more difficult to remove following decellularization, raising cytotoxicity concerns[74,118,119]. The decellularization protocol included freeze-thaw cycles in a hypotonic solution to promote cell lysis followed by 1% Triton X-100 detergent extraction and digestion with DNase and RNase to extract cellular components, and finally, extensive washing to remove residual detergent and cellular debris. This protocol was highly effective at extracting nucleic acids from the tissues as determined by DAPI staining and quantification of double-stranded DNA (dsDNA) content, supporting that the tissues were effectively decellularized. More specifically, the protocol resulted in a ~92% reduction in the dsDNA content, which is similar to other protocols in the literature that used the ionic detergent SDS (~95% reduction) or the non-ionic detergent Triton X-100 (~94% reduction) to decellularize mouse small intestine[81].

Collagen is the primary structural protein in the small intestine and it is known to play an important role in regulating the function of intestinal epithelial cells[7,11,15]. Thus, it is critical that a decellularization protocol is able to retain collagen[7]. Analysis of collagen content via picrosirius red staining and the hydroxyproline assay indicated that there was a relative enrichment in collagen content at the end of processing. These findings are consistent with previous reports in the literature and are consistent with the loss of cells and other ECM components during processing[56,85].

We additionally measured the retention of GAGs in our decellularized tissue, as GAGs can sequester growth factors and play a key role in maintaining tissue hydration as a result of their hydrophilic nature[7,120]. In addition, cells can also interact directly with GAGs through cell surface receptors, which can modulate cellular processes including intestinal crypt homeostasis[7,32,35]. Thus, augmenting GAG retention may enhance the bioactivity of decellularized tissues. Based on toluidine blue staining and the dimethylmethylene blue (DMMB) assay, the novel protocol developed in this thesis was favorable for GAG retention, with no significant difference between the decellularized and native tissue samples observed. In contrast, previous studies have shown a significant loss in GAG content following increased sodium deoxycholate cycles in rat small intestine, and another study reported only ~42% GAG retention following sodium dodecyl sulphate treatment in porcine small intestine, potentially linked to the use of stronger ionic detergents[85,89].

Immunohistochemical staining confirmed the presence of collagen types I and IV, fibronectin, and laminin within the decellularized tissue samples at the end of processing. Collagen I and IV are known to be distributed throughout the ECM in the small intestine[7]. Collagen I defines the tissue structure, while collagen IV is integral to the basement membrane, where it is in direct contact with epithelial and mesenchymal cells and is important for the regulation of epithelial cell homeostasis[7,15] Fibronectin is an important mediator of cell-matrix interactions and can regulate cell functions including cell proliferation, adhesion, and differentiation[7,24–26]. Similarly, laminin is another abundant glycoprotein found in the intestinal crypt membrane, which can regulate the function of the intestinal epithelium, including promoting cell adhesion and directing

differentiation[21,22]. Interestingly, Gjorevski *et al* previously showed that the addition of laminin and fibronectin to polyethylene glycol (PEG) hydrogels *in vitro* enhanced mouse ISC proliferation and survival, supporting that the retention of these components within our DSI may be favorable for organoid growth[102].

For intestinal organoid culture, there is specific interest in the development of hydrogel platforms that can encapsulate cells with high viability within a 3D microenvironment that mimics the native small ISC niche[57]. To generate such platforms, decellularized tissue can be enzymatically digested to obtain polypeptide solutions that can subsequently be induced to form hydrogels by promoting the self-assembly of the remaining collagen fibrils[56,57,99]. In this study, a protocol was established to make hydrogels from pepsin-digested intestinal ECM prepared with the decellularized mouse tissues. A wide range of pepsin-digestion protocols have been reported in the literature for tissue sources including adipose tissue, bone, cartilage, colon, small intestine, and heart tissue[56,57,94–98]. Notably, pepsin digestion requires careful optimization as the peptide solution generated can be affected by multiple factors including digestion time, pH, enzyme concentration, substrate concentration, temperature, and agitation[57], which can impact hydrogel formation. The finalized protocol developed in this thesis involved 24 hours of digestion at room temperature, with 1 mg/mL pepsin and an ECM concentration of 25 mg/mL. Increasing the temperature to 37ºC during digestion, or decreasing the ECM concentration to 10 mg/mL resulted in unstable hydrogel formation, likely due to over-digestion of the ECM. Similarly, increasing the ECM concentration to 50 mg/mL resulted in ineffective digestion. Interestingly, others have reported fabricating stable intestinal-derived hydrogels with ECM concentrations as low as 6 mg/mL using decellularized porcine tissues[56,57]. This difference in hydrogel stability could be attributed to species-specific differences in the ECM composition and could also be influenced by the specific decellularization protocols used.

As a first step in testing the new intestinal ECM-derived hydrogel platform, a simple cell culture model involving the murine 3T3 fibroblast cell line was used to verify that the pepsin-digested intestinal ECM supported cell viability and had bioactive effects on encapsulated cell populations. Positively, LIVE/DEAD staining indicated that the DSI

provided cell adhesive cues that supported cell spreading over time[121], and the MTT results indicated that there was cell expansion over time, similar to Matrigel®. Our findings are consistent with a previous study that showed high viability and cell spreading in 3T3 cells encapsulated and cultured in type I collagen hydrogels over 6 days[122]. Similarly, another study reported high viability, cell growth, and cell spreading of 3T3 cells following encapsulation and 7 days of culture within ECM-derived hydrogels comprised of pepsin-digested decellularized porcine dermis or decellularized urinary bladder[123]. Overall, these findings support the cell-supportive nature of ECM-derived hydrogels fabricated from pepsin-digested ECM.

When intestinal organoids were encapsulated within the DSI hydrogels and cultured for 14 days, similar growth patterns were observed as compared to the Matrigel® controls, with budding structures including granule-containing cells, consistent with Paneth cells[36], observed starting at 7 days. Additionally, H&E staining of organoids grown in DSI versus Matrigel® revealed similar structures with an epithelial cell monolayer with budding crypts surrounding a central lumen. These findings are consistent with the work of Clevers and colleagues, who developed ECM-derived hydrogels comprised of pepsin-digested decellularized porcine small intestine and showed that they could support the growth of human and mouse-derived small intestinal organoids[56]. More specifically, their quantitative analyses of size based on brightfield imaging also revealed that the mouse and human intestinal organoids showed similar growth in their hydrogels to those cultured in Matrigel®. Further, their study revealed that intestinal organoids could be maintained over several passages, but they noted a decrease in the quality of the morphology of their human organoids over multiple passages, based on brightfield imaging. Similarly, in our current study, intestinal organoids passaged from DSI back into fresh DSI or Matrigel® revealed that the organoids passaged into the DSI hydrogels grew noticeably slower compared to those passaged into Matrigel®. Additional studies focused on compositional analyses of Matrigel® and DSI are needed to determine if there are growth factors present in Matrigel® which are absent in the DSI. Additionally, mechanical properties such as gel stiffness may be playing a role in the regulation of the

ISCs and can be evaluated by performing compression testing using a CellScale MicroTester system to measure the Young's Modulus of the gels.

While the DSI hydrogels showed favorable cell supportive qualities including the ability to support the growth of established organoids, there were some technical disadvantages noted with their use, including that they were less transparent than Matrigel®, which made imaging more challenging. Furthermore, unlike Matrigel®, the DSI hydrogels were not thermally reversible and required mechanical disruption to passage the intestinal organoids. Therefore, additional studies focused on degrading the ECM before passaging may aid in the successful passaging of DSI-grown organoids. In addition, the hydrogels did not consistently adhere to the tissue culture plates, making it more difficult to track specific organoids by microscopy over time. To try to address these limitations, the final goal of this study was to investigate composite alginate + DSI hydrogels, with the goal of creating a more structurally robust and tunable platform that integrated the bioactivity of the intestinal-derived ECM[124]. Alginate was selected as the base material as it has reversible gelation properties that are advantageous for cell extraction[124]. It is also well known to support the viability of encapsulated cells *in vitro*[59,60].

In the current study, the incorporation of pepsin-digested ECM sourced from the DSI or decellularized porcine meniscus as a control was shown to promote the spreading and growth of encapsulated 3T3 fibroblasts relative to alginate alone controls. These findings are consistent with previous studies in the literature on the incorporation of ECM proteins within alginate[122]. For example, Liu *et al.* observed that the incorporation of type I collagen into alginate hydrogels promoted high viability on day 6 relative to day 0, and cell spreading of 3T3 cells based on LIVE/DEAD staining at 6 days post-encapsulation[122]. Overall, these findings indicate that the incorporation of ECM peptides within alginate can provide biological cues needed to support cell attachment and growth[59].

However, when mouse intestinal organoids were encapsulated within the alginate-based hydrogels, no cell growth was observed over the 14 day culture period. In a previous study, alginate hydrogels were shown to support the growth of organoids derived from

human induced pluripotent stem cells (iPSCs) when cultured with the addition of mesenchymal supporting cells and growth factors including epidermal growth factor (EGF), R-Spondin2, and Noggin-Fc[59]. However, the number of spheroids that gave rise to organoids was lower in all alginate concentrations relative to Matrigel® on day 28 post-encapsulation. Notably, organoids derived from iPSCs are distinct from organoids grown from primary adult tissues, although they may provide a basis for optimizing growth conditions for primary organoids. Importantly, the authors reported that varying the alginate concentration (0.5%, 1%, 2%, 3%, and 4% alginate) affected organoid viability and growth, with enhanced viability in the 1% and 2% alginate concentrations. These findings suggest that it may be possible to tune our composite alginate platform to better support intestinal organoid growth, and future studies could explore varying other parameters such as the final ECM concentration within the gels or the addition of other growth factors and/or co-culture with mesenchymal stromal cell[46,125].

4.1   Conclusion and Significance

In summary, a new decellularization protocol was developed for mouse small intestine. The decellularization protocol was confirmed to effectively remove cellular content while preserving key ECM constituents present in the native small intestine including GAGs, collagens, fibronectin, and laminin. A protocol was subsequently developed to fabricate intestinal ECM-derived hydrogels from pepsin-digested DSI. Hydrogels comprised exclusively of ECM showed bioactive effects on encapsulated 3T3 cells and demonstrated their ability to promote primary mouse intestinal organoid growth similar to Matrigel®. Composite hydrogels were formed by incorporating pepsin-digested DSI within alginate. The inclusion of the ECM within the composite gels was shown to have bioactive effects on encapsulated 3T3 cells relative to alginate alone. While the alginate-based hydrogels were successfully used to encapsulate intestinal organoids, no detectable organoid growth was noted over the 14 day culture period, suggesting that further optimization of the platform was necessary for this application. Overall, this body of work provides insight into how tissue-specific ECM can be used as a bioscaffold for supporting and promoting ISC growth.

4.2   Implications and Future Directions

This thesis developed two novel intestinal ECM-derived hydrogel platforms and serves as a basis for strategies seeking to harness the intestinal-derived ECM for the culture of mouse intestinal organoids. These hydrogels showed promise as a starting point for replacing Matrigel® as the matrix for culturing intestinal organoids, and may also prove to be a useful tool for *in vivo* cell delivery in future applications. Future studies should focus on further characterizing the organoids cultured within these novel hydrogel platforms, including identifying the cell types present. This can be done by histologic analyses and immunofluorescent labelling of specific cell types and comparison to organoids grown in Matrigel®.

Further investigation of the proteins and growth factors present in the decellularized small intestine and the hydrogels fabricated from the pepsin-digested DSI relative to Matrigel® would also be recommended. Compositional analysis may help to identify specific proteins involved in regulating ISC growth and organoid formation. One approach would be to conduct in-depth proteomic analyses using high throughput mass spectrometry techniques to identify proteins present and their relative abundance within the ECM-derived materials[56,126]. Currently, Matrigel®-based cultures require the addition of growth factors including R-spondin, Noggin, and EGF to enable organoid formation and growth[36]. Therefore, compositional analyses may allow us to identify growth factors that may be present in DSI versus Matrigel®, or conversely, factors that are present in Matrigel® but not DSI, and subsequently explore the removal/addition of those factors in the DSI hydrogel organoid cultures.

One of the disadvantages of the DSI hydrogels versus Matrigel® is the optical clarity, as the DSI hydrogels were not fully transparent. This resulted in challenges with bright-field imaging of specific cells within the organoids. The ECM-based hydrogels also occasionally floated freely within the media, which was not ideal for imaging. Potential approaches to address these barriers would be to make adjustments to the pepsin digestion protocol, such as varying the ECM concentration or removing undigested materials to reduce particulates. However, these changes may also impact the structure

and composition of the ECM and ultimately its ability to promote organoid growth, so further cell culture studies would be needed to confirm bioactivity if there are changes in the ECM processing methods.

Matrigel®-grown intestinal organoids are known to remain highly viable over many passages. Thus, it would be interesting to explore whether the same viability is also attainable for organoids grown in intestinal-ECM-derived organoids. The shear stress on the DSI-grown organoids during passaging and the residual DSI remaining after passaging could have affected their viability in the fresh DSI hydrogels. Treatment of the DSI hydrogels with collagenase or cell recovery solution could aid in the release of cells from the DSI hydrogels during passaging and reduce the potential damage to the organoids caused by mechanical disruption which may be inhibiting organoid growth[56,127].

An additional focus of future studies should be directed towards enhancing the ability of the alginate + DSI hydrogels to promote intestinal organoid growth and further characterizing the capacity of the platform to support organoid survival. Other ways to assess if organoids are viable are the LIVE/DEAD assay. Additionally, organoids could be released from the alginate and resuspended in Matrigel® to assess their viability. Furthermore, alterations in the composition of the alginate + DSI may need to be explored. Increasing the DSI concentration while decreasing the alginate concentration may prove to be beneficial for providing the appropriate biochemical cues needed to promote intestinal organoid growth, similar to the DSI alone gels. Similar to the DSI alone gels, additional factors may be required which may already be present in Matrigel®, but not DSI. Therefore, exploring the addition of other growth factors or a co-culture model with mesenchymal stromal cells, which can provide necessary growth factors, may be required for the ISCs to expand and develop into intestinal organoids in the composite alginate gels[46,125].

The intestinal ECM has been demonstrated to provide biochemical cues capable of supporting and promoting intestinal organoid growth. The need for tissue-specific ECM, however, may require further investigation. The Clevers' group provided evidence that

porcine intestinal ECM hydrogels can promote the growth of organoids derived from various endodermal tissues. Therefore, there is a need to explore if tissue-specific ECM is required for intestinal organoid growth or if ECM derived from other tissues could similarly support organoid growth. Finally, characterization of the organoids cultured within ECM derived from other tissues may reveal whether important biological differences in the properties of ECM derived from the intestine versus other tissues exist.

References

1. Collins JT, Badireddy M. Anatomy, Abdomen and Pelvis, Small Intestine. In: StatPearls [Internet]. Treasure Island (FL): StatPearls Publishing; 2020 [cited 2020 Mar 20]. Available from: http://www.ncbi.nlm.nih.gov/books/NBK459366/

2. Greaves P. Chapter 8 - Digestive System. In: Greaves P, editor. Histopathology of Preclinical Toxicity Studies (Fourth Edition) [Internet]. Boston: Academic Press; 2012 [cited 2020 Mar 22]. p. 325–431. Available from: http://www.sciencedirect.com/science/article/pii/B9780444538567000087

3. Kong S, Zhang YH, Zhang W. Regulation of Intestinal Epithelial Cells Properties and Functions by Amino Acids [Internet]. Vol. 2018, BioMed Research International. Hindawi; 2018 [cited 2020 Mar 21]. p. e2819154. Available from: https://www.hindawi.com/journals/bmri/2018/2819154/

4. Haber AL, Biton M, Rogel N, Herbst RH, Shekhar K, Smillie C, et al. A single-cell survey of the small intestinal epithelium. Nature. 2017 Nov;551(7680):333–9.

5. Gassler N. Paneth cells in intestinal physiology and pathophysiology. World J Gastrointest Pathophysiol. 2017 Nov 15;8(4):150–60.

6. Moran-Ramos S, Tovar AR, Torres N. Diet: Friend or Foe of Enteroendocrine Cells: How It Interacts with Enteroendocrine Cells. Adv Nutr. 2012 Jan 1;3(1):8–20.

7. Meran L, Baulies A, Li VSW. Intestinal Stem Cell Niche: The Extracellular Matrix and Cellular Components. Stem Cells Int. 2017;2017:1–11.

8. Gerbe F, Legraverend C, Jay P. The intestinal epithelium tuft cells: specification and function. Cell Mol Life Sci. 2012;69(17):2907–17.

9. Middelhoff M, Westphalen CB, Hayakawa Y, Yan KS, Gershon MD, Wang TC, et al. Dclk1-expressing tuft cells: critical modulators of the intestinal niche? Am J Physiol-Gastrointest Liver Physiol. 2017 Oct 1;313(4):G285–99.

10. Umar S. Intestinal Stem Cells. Curr Gastroenterol Rep. 2010 Oct;12(5):340–8.

11. Shoulders MD, Raines RT. Collagen Structure and Stability. Annu Rev Biochem. 2009 Jun 1;78(1):929–58.

12. Frantz C, Stewart KM, Weaver VM. The extracellular matrix at a glance. J Cell Sci. 2010 Dec 15;123(24):4195–200.

13. Pawelec KM, Best SM, Cameron RE. Collagen: a network for regenerative medicine. J Mater Chem B. 2016 Oct 12;4(40):6484–96.

14. Zeng Y-J, Qiao A-K, Yu J-D, Zhao J-B, Liao D-H, Xu X-H, et al. Collagen fiber angle in the submucosa of small intestine and its application in gastroenterology. World J Gastroenterol WJG. 2003 Apr 15;9(4):804–7.

15. Cescon M, Gattazzo F, Chen P, Bonaldo P. Collagen VI at a glance. J Cell Sci. 2015 Oct 1;128(19):3525–31.

16. Gelse K, Pöschl E, Aigner T. Collagens—structure, function, and biosynthesis. Adv Drug Deliv Rev. 2003 Nov 28;55(12):1531–46.

17. Knupp C, Squire JM. Molecular Packing in Network-Forming Collagens. Sci World J. 2003;3:558–77.

18. Singh P, Carraher C, Schwarzbauer JE. Assembly of Fibronectin Extracellular Matrix. Annu Rev Cell Dev Biol. 2010 Oct 6;26(1):397–419.

19. Teller IC, Beaulieu J-F. Interactions between laminin and epithelial cells in intestinal health and disease. Expert Rev Mol Med. 2001 Sep;3(24):1–18.

20. Beck K, Hunter I, Engel J. Structure and function of laminin: anatomy of a multidomain glycoprotein. FASEB J. 1990 Feb 1;4(2):148–60.

21. Hamill KJ, Kligys K, Hopkinson SB, Jones JCR. Laminin deposition in the extracellular matrix: a complex picture emerges. J Cell Sci. 2009 Dec 15;122(24):4409–17.

22. Mahoney ZX, Stappenbeck TS, Miner JH. Laminin α5 influences the architecture of the mouse small intestine mucosa. J Cell Sci. 2008 Aug 1;121(15):2493–502.

23. Simon-Assmann P, Spenle C, Lefebvre O, Kedinger M. Chapter 8 - The Role of the Basement Membrane as a Modulator of Intestinal Epithelial–Mesenchymal Interactions. In: Kaestner KH, editor. Progress in Molecular Biology and Translational Science [Internet]. Academic Press; 2010 [cited 2020 Mar 25]. p. 175–206. Available from: http://www.sciencedirect.com/science/article/pii/B9780123812803000087

24. Beaulieu J-F, Vachon PH, Chartrand S. Immunolocalization of extracellular matrix components during organogenesis in the human small intestine. Anat Embryol (Berl). 1991 Apr 1;183(4):363–9.

25. Hynes RO. The Extracellular Matrix: Not Just Pretty Fibrils. Science. 2009 Nov 27;326(5957):1216–9.

26. Kolachala VL, Bajaj R, Wang L, Yan Y, Ritzenthaler JD, Gewirtz AT, et al. Epithelial-derived Fibronectin Expression, Signaling, and Function in Intestinal Inflammation. J Biol Chem. 2007 Nov 9;282(45):32965–73.

27. Quaroni A, Isselbacher KJ, Ruoslahti E. Fibronectin synthesis by epithelial crypt cells of rat small intestine. Proc Natl Acad Sci. 1978 Nov 1;75(11):5548–52.

28. To WS, Midwood KS. Plasma and cellular fibronectin: distinct and independent functions during tissue repair. Fibrogenesis Tissue Repair. 2011 Sep 16;4(1):21.

29. Gandhi NS, Mancera RL. The Structure of Glycosaminoglycans and their Interactions with Proteins. Chem Biol Drug Des. 2008;72(6):455–82.

30. Meran L, Baulies A, Li VSW. Intestinal Stem Cell Niche: The Extracellular Matrix and Cellular Components. Stem Cells Int. 2017;2017:1–11.

31. Sherman L, Sleeman J, Herrlich P, Ponta H. Hyaluronate receptors: key players in growth, differentiation, migration and tumor progression. Curr Opin Cell Biol. 1994 Oct 1;6(5):726–33.

32. de la Motte CA. Hyaluronan in intestinal homeostasis and inflammation: implications for fibrosis. Am J Physiol - Gastrointest Liver Physiol. 2011 Dec;301(6):G945–9.

33. Fuerer C, Habib SJ, Nusse R. A study on the interactions between heparan sulfate proteoglycans and Wnt proteins. Dev Dyn. 2010;239(1):184–90.

34. Murch SH, MacDonald TT, Walker-Smith JA, Lionetti P, Levin M, Klein NJ. Disruption of sulphated glycosaminoglycans in intestinal inflammation. The Lancet. 1993 Mar 20;341(8847):711–4.

35. Yamamoto S, Nakase H, Matsuura M, Honzawa Y, Matsumura K, Uza N, et al. Heparan sulfate on intestinal epithelial cells plays a critical role in intestinal crypt homeostasis via Wnt/β-catenin signaling. Am J Physiol - Gastrointest Liver Physiol. 2013 Aug 1;305(3):G241–9.

36. Sato T, Vries RG, Snippert HJ, van de Wetering M, Barker N, Stange DE, et al. Single Lgr5 stem cells build crypt-villus structures in vitro without a mesenchymal niche. Nature. 2009 May;459(7244):262–5.

37. Simian M, Bissell MJ. Organoids: A historical perspective of thinking in three dimensions. J Cell Biol. 2017 Jan 2;216(1):31–40.

38. Rossi G, Manfrin A, Lutolf MP. Progress and potential in organoid research. Nat Rev Genet. 2018 Nov;19(11):671–87.

39. BR27117-Culturing_Intestinal_Organoids.pdf [Internet]. [cited 2020 Apr 8]. Available from: https://cdn.stemcell.com/media/files/brochure/BR27117-Culturing_Intestinal_Organoids.pdf

40. Fair KL, Colquhoun J, Hannan NRF. Intestinal organoids for modelling intestinal development and disease. Philos Trans R Soc B Biol Sci. 2018 Jul 5;373(1750):20170217.

41. Sato T, Stange DE, Ferrante M, Vries RGJ, Van Es JH, Van den Brink S, et al. Long-term expansion of epithelial organoids from human colon, adenoma, adenocarcinoma, and Barrett's epithelium. Gastroenterology. 2011 Nov;141(5):1762–72.

42. Haramis A-PG, Begthel H, van den Born M, van Es J, Jonkheer S, Offerhaus GJA, et al. De novo crypt formation and juvenile polyposis on BMP inhibition in mouse intestine. Science. 2004 Mar 12;303(5664):1684–6.

43. Kim K-A, Kakitani M, Zhao J, Oshima T, Tang T, Binnerts M, et al. Mitogenic influence of human R-spondin1 on the intestinal epithelium. Science. 2005 Aug 19;309(5738):1256–9.

44. Dignass AU, Sturm A. Peptide growth factors in the intestine. Eur J Gastroenterol Hepatol. 2001 Jul;13(7):763–70.

45. Sato T, van Es JH, Snippert HJ, Stange DE, Vries RG, van den Born M, et al. Paneth cells constitute the niche for Lgr5 stem cells in intestinal crypts. Nature. 2011 Jan 20;469(7330):415–8.

46. Spence JR, Mayhew CN, Rankin SA, Kuhar M, Vallance JE, Tolle K, et al. Directed differentiation of human pluripotent stem cells into intestinal tissue in vitro. Nature. 2011 Feb 3;470(7332):105–9.

47. Tsai Y-H, Nattiv R, Dedhia PH, Nagy MS, Chin AM, Thomson M, et al. *In vitro* patterning of pluripotent stem cell-derived intestine recapitulates *in vivo* human development. Development. 2017 Mar 15;144(6):1045–55.

48. Martin LY, Ladd MR, Werts A, Sodhi CP, March JC, Hackam DJ. Tissue engineering for the treatment of short bowel syndrome in children. Pediatr Res. 2018 Jan;83(1–2):249–57.

49. Creff J, Malaquin L, Besson A. In vitro models of intestinal epithelium: Toward bioengineered systems. J Tissue Eng. 2021 Jan 1;12:2041731420985202.

50. Antfolk M, Jensen KB. A bioengineering perspective on modelling the intestinal epithelial physiology in vitro. Nat Commun. 2020 Dec 7;11(1):6244.

51. Kleinman HK, Martin GR. Matrigel: Basement membrane matrix with biological activity. Semin Cancer Biol. 2005 Oct 1;15(5):378–86.

52. Aisenbrey EA, Murphy WL. Synthetic alternatives to Matrigel. Nat Rev Mater. 2020 Jul;5(7):539–51.

53. Bahram M, Mohseni N, Moghtader M. An Introduction to Hydrogels and Some Recent Applications. Emerg Concepts Anal Appl Hydrogels [Internet]. 2016 Aug 24 [cited 2020 May 12]; Available from: https://www.intechopen.com/books/emerging-

concepts-in-analysis-and-applications-of-hydrogels/an-introduction-to-hydrogels-and-some-recent-applications

54. Silva AKA, Richard C, Bessodes M, Scherman D, Merten O-W. Growth Factor Delivery Approaches in Hydrogels. Biomacromolecules. 2009 Jan 12;10(1):9–18.

55. Catoira MC, Fusaro L, Di Francesco D, Ramella M, Boccafoschi F. Overview of natural hydrogels for regenerative medicine applications. J Mater Sci Mater Med. 2019 Oct 10;30(10):115.

56. Giobbe GG, Crowley C, Luni C, Campinoti S, Khedr M, Kretzschmar K, et al. Extracellular matrix hydrogel derived from decellularized tissues enables endodermal organoid culture. Nat Commun. 2019 Dec 11;10(1):1–14.

57. Saldin LT, Cramer MC, Velankar SS, White LJ, Badylak SF. Extracellular matrix hydrogels from decellularized tissues: Structure and function. Acta Biomater. 2017 Feb 1;49:1–15.

58. Cruz-Acuña R, Quirós M, Farkas AE, Dedhia PH, Huang S, Siuda D, et al. Synthetic Hydrogels for Human Intestinal Organoid Generation and Colonic Wound Repair. Nat Cell Biol. 2017 Nov;19(11):1326–35.

59. Capeling MM, Czerwinski M, Huang S, Tsai Y-H, Wu A, Nagy MS, et al. Nonadhesive Alginate Hydrogels Support Growth of Pluripotent Stem Cell-Derived Intestinal Organoids. Stem Cell Rep. 2019 Feb 12;12(2):381–94.

60. Lee KY, Mooney DJ. Alginate: Properties and biomedical applications. Prog Polym Sci. 2012 Jan 1;37(1):106–26.

61. Aramwit P. Introduction to biomaterials for wound healing. In: Wound Healing Biomaterials [Internet]. Elsevier; 2016 [cited 2020 May 12]. p. 3–38. Available from: https://linkinghub.elsevier.com/retrieve/pii/B9781782424567000015

62. Wu Z, Su X, Xu Y, Kong B, Sun W, Mi S. Bioprinting three-dimensional cell-laden tissue constructs with controllable degradation. Sci Rep. 2016 Apr 19;6(1):24474.

63. Rinaudo M. Biomaterials based on a natural polysaccharide: alginate. TIP. 2014 Jun 1;17(1):92–6.

64. Nakamura N, Kimura T, Kishida A. Overview of the Development, Applications, and Future Perspectives of Decellularized Tissues and Organs. ACS Biomater Sci Eng. 2017 Jul 10;3(7):1236–44.

65. Yu Y, Alkhawaji A, Ding Y, Mei J. Decellularized scaffolds in regenerative medicine. Oncotarget. 2016 Jul 29;7(36):58671–83.

66. Gilbert TW, Sellaro TL, Badylak SF. Decellularization of tissues and organs. Biomaterials. 2006 Jul 1;27(19):3675–83.

67. Crapo PM, Gilbert TW, Badylak SF. An overview of tissue and whole organ decellularization processes. Biomaterials. 2011 Apr 1;32(12):3233–43.

68. Chen F, Yoo JJ, Atala A. Acellular collagen matrix as a possible "off the shelf" biomaterial for urethral repair. Urology. 1999 Sep 1;54(3):407–10.

69. Sawkins MJ, Bowen W, Dhadda P, Markides H, Sidney LE, Taylor AJ, et al. Hydrogels derived from demineralized and decellularized bone extracellular matrix. Acta Biomater. 2013 Aug;9(8):7865–73.

70. Flynn LE. The use of decellularized adipose tissue to provide an inductive microenvironment for the adipogenic differentiation of human adipose-derived stem cells. Biomaterials. 2010 Jun;31(17):4715–24.

71. Metcalf MH, Savoie FH, Kellum B. Surgical technique for xenograft (SIS) augmentation of rotator-cuff repairs. Oper Tech Orthop. 2002 Jan 1;12(3):204–8.

72. Gilbert TW. Strategies for tissue and organ decellularization. J Cell Biochem. 2012 Jul 1;113(7):2217–22.

73. Gilpin A, Yang Y. Decellularization Strategies for Regenerative Medicine: From Processing Techniques to Applications. BioMed Res Int. 2017 Apr 30;2017:e9831534.

74. Syed O, Walters NJ, Day RM, Kim H-W, Knowles JC. Evaluation of decellularization protocols for production of tubular small intestine submucosa scaffolds for use in oesophageal tissue engineering. Acta Biomater. 2014 Dec 1;10(12):5043–54.

75. Decellularized matrices for tissue engineering: Expert Opinion on Biological Therapy: Vol 10, No 12 [Internet]. [cited 2020 Apr 12]. Available from: https://www.tandfonline.com/doi/full/10.1517/14712598.2010.534079?casa_token=e pXA6Ot3wwEAAAAA:-jGnZvNqJ8W5GTAndsjTA83rpD7lv9KmbeaFDCcQ57aSqO-oefH36rJLoOz_-MdYvBdhJ8iKk3lmKxg

76. Aamodt JM, Grainger DW. Extracellular matrix-based biomaterial scaffolds and the host response. Biomaterials. 2016 Apr 1;86:68–82.

77. Robb KP, Shridhar A, Flynn LE. Decellularized Matrices As Cell-Instructive Scaffolds to Guide Tissue-Specific Regeneration. ACS Biomater Sci Eng. 2018 Nov 12;4(11):3627–43.

78. Nagata S, Hanayama R, Kawane K. Autoimmunity and the Clearance of Dead Cells. Cell. 2010 Mar 5;140(5):619–30.

79. Zheng MH, Chen J, Kirilak Y, Willers C, Xu J, Wood D. Porcine small intestine submucosa (SIS) is not an acellular collagenous matrix and contains porcine DNA:

possible implications in human implantation. J Biomed Mater Res B Appl Biomater. 2005 Apr;73(1):61–7.

80. Ahn SJ, Costa J, Rettig Emanuel J. PicoGreen Quantitation of DNA: Effective Evaluation of Samples Pre-or Psost-PCR. Nucleic Acids Res. 1996 Jul 1;24(13):2623–5.

81. Oliveira AC, Garzón I, Ionescu AM, Carriel V, Cardona J de la C, González-Andrades M, et al. Evaluation of Small Intestine Grafts Decellularization Methods for Corneal Tissue Engineering. PLOS ONE. 2013 Jun 14;8(6):e66538.

82. Eitan Y, Sarig U, Dahan N, Machluf M. Acellular Cardiac Extracellular Matrix as a Scaffold for Tissue Engineering: *In Vitro* Cell Support, Remodeling, and Biocompatibility. Tissue Eng Part C Methods. 2010 Aug;16(4):671–83.

83. Wang RM, Christman KL. Decellularized myocardial matrix hydrogels: In basic research and preclinical studies. Adv Drug Deliv Rev. 2016 Jan 15;96:77–82.

84. Morissette Martin P, Grant A, Hamilton DW, Flynn LE. Matrix composition in 3-D collagenous bioscaffolds modulates the survival and angiogenic phenotype of human chronic wound dermal fibroblasts. Acta Biomater. 2019 Jan 1;83:199–210.

85. Totonelli G, Maghsoudlou P, Garriboli M, Riegler J, Orlando G, Burns AJ, et al. A rat decellularized small bowel scaffold that preserves villus-crypt architecture for intestinal regeneration. Biomaterials. 2012 Apr 1;33(12):3401–10.

86. Kuljanin M, Brown CFC, Raleigh MJ, Lajoie GA, Flynn LE. Collagenase treatment enhances proteomic coverage of low-abundance proteins in decellularized matrix bioscaffolds. Biomaterials. 2017 Nov 1;144:130–43.

87. Li Q, Uygun BE, Geerts S, Ozer S, Scalf M, Gilpin SE, et al. Proteomic analysis of naturally-sourced biological scaffolds. Biomaterials. 2016 Jan 1;75:37–46.

88. Maghsoudlou P, Totonelli G, Loukogeorgakis SP, Eaton S, De Coppi P. A Decellularization Methodology for the Production of a Natural Acellular Intestinal Matrix. J Vis Exp JoVE [Internet]. 2013 Oct 7 [cited 2020 Apr 22];(80). Available from: https://www.ncbi.nlm.nih.gov/pmc/articles/PMC3923547/

89. Nowocin AK, Southgate A, Gabe SM, Ansari T. Biocompatibility and potential of decellularized porcine small intestine to support cellular attachment and growth. J Tissue Eng Regen Med. 2016;10(1):E23-33.

90. White LJ, Taylor AJ, Faulk DM, Keane TJ, Saldin LT, Reing JE, et al. The impact of detergents on the tissue decellularization process: A ToF-SIMS study. Acta Biomater. 2017 Mar 1;50:207–19.

91. Hussey GS, Cramer MC, Badylak SF. Extracellular Matrix Bioscaffolds for Building Gastrointestinal Tissue. Cell Mol Gastroenterol Hepatol. 2018 Jan 1;5(1):1–13.

92. Kornmuller A, Brown CFC, Yu C, Flynn LE. Fabrication of Extracellular Matrix-derived Foams and Microcarriers as Tissue-specific Cell Culture and Delivery Platforms. J Vis Exp JoVE. 2017 Apr 11;(122):55436.

93. Rezakhani S, Gjorevski N, Lutolf MP. Extracellular matrix requirements for gastrointestinal organoid cultures. Biomaterials. 2021 Sep 1;276:121020.

94. Sawkins MJ, Bowen W, Dhadda P, Markides H, Sidney LE, Taylor AJ, et al. Hydrogels derived from demineralized and decellularized bone extracellular matrix. Acta Biomater. 2013 Aug 1;9(8):7865–73.

95. Young DA, Ibrahim DO, Hu D, Christman KL. Injectable hydrogel scaffold from decellularized human lipoaspirate. Acta Biomater. 2011 Mar 1;7(3):1040–9.

96. Singelyn JM, DeQuach JA, Seif-Naraghi SB, Littlefield RB, Schup-Magoffin PJ, Christman KL. Naturally derived myocardial matrix as an injectable scaffold for cardiac tissue engineering. Biomaterials. 2009 Oct 1;30(29):5409–16.

97. Keane TJ, Dziki J, Castelton A, Faulk DM, Messerschmidt V, Londono R, et al. Preparation and characterization of a biologic scaffold and hydrogel derived from colonic mucosa. J Biomed Mater Res B Appl Biomater. 2017;105(2):291–306.

98. Pati F, Jang J, Ha D-H, Won Kim S, Rhie J-W, Shim J-H, et al. Printing three-dimensional tissue analogues with decellularized extracellular matrix bioink. Nat Commun. 2014 Jun 2;5(1):3935.

99. Manka SW, Carafoli F, Visse R, Bihan D, Raynal N, Farndale RW, et al. Structural insights into triple-helical collagen cleavage by matrix metalloproteinase 1. Proc Natl Acad Sci. 2012 Jul 31;109(31):12461–6.

100. Jabaji Z, Sears CM, Brinkley GJ, Lei NY, Joshi VS, Wang J, et al. Use of Collagen Gel as an Alternative Extracellular Matrix for the In Vitro and In Vivo Growth of Murine Small Intestinal Epithelium. Tissue Eng Part C Methods. 2013 Dec;19(12):961–9.

101. Jee JH, Lee DH, Ko J, Hahn S, Jeong SY, Kim HK, et al. Development of Collagen-Based 3D Matrix for Gastrointestinal Tract-Derived Organoid Culture. Stem Cells Int. 2019 Jun 13;2019:e8472712.

102. Gjorevski N, Sachs N, Manfrin A, Giger S, Bragina ME, Ordóñez-Morán P, et al. Designer matrices for intestinal stem cell and organoid culture. Nature. 2016 Nov;539(7630):560–4.

103. Zhao Z, Vizetto-Duarte C, Moay ZK, Setyawati MI, Rakshit M, Kathawala MH, et al. Composite Hydrogels in Three-Dimensional in vitro Models. Front Bioeng Biotechnol [Internet]. 2020 [cited 2021 Oct 21];0. Available from: https://www.frontiersin.org/articles/10.3389/fbioe.2020.00611/full

104.   Beaulieu JF. Integrins and human intestinal cell functions. Front Biosci. 1999 Mar 1;4:D310-21.

105.   Gattazzo F, Urciuolo A, Bonaldo P. Extracellular matrix: A dynamic microenvironment for stem cell niche. Biochim Biophys Acta BBA - Gen Subj. 2014 Aug 1;1840(8):2506–19.

106.   Jones RG, Li X, Gray PD, Kuang J, Clayton F, Samowitz WS, et al. Conditional deletion of β1 integrins in the intestinal epithelium causes a loss of Hedgehog expression, intestinal hyperplasia, and early postnatal lethality. J Cell Biol. 2006 Nov 6;175(3):505–14.

107.   Onfroy-Roy L, Hamel D, Foncy J, Malaquin L, Ferrand A. Extracellular Matrix Mechanical Properties and Regulation of the Intestinal Stem Cells: When Mechanics Control Fate. Cells. 2020 Dec;9(12):2629.

108.   Simon-Assmann P, Duclos B, Orian-Rousseau V, Arnold C, Mathelin C, Engvall E, et al. Differential expression of laminin isoforms and α6-β4 integrin subunits in the developing human and mouse intestine. Dev Dyn. 1994;201(1):71–85.

109.   Beaulieu JF. Differential expression of the VLA family of integrins along the crypt-villus axis in the human small intestine. J Cell Sci. 1992 Jul 1;102(3):427–36.

110.   Ricard-Blum S, Salza R. Matricryptins and matrikines: biologically active fragments of the extracellular matrix. Exp Dermatol. 2014;23(7):457–63.

111.   Mauney J, Olsen BR, Volloch V. Matrix remodeling as stem cell recruitment event: A novel in vitro model for homing of human bone marrow stromal cells to the site of injury shows crucial role of extracellular collagen matrix. Matrix Biol. 2010 Oct 1;29(8):657–63.

112.   Davis GE, Bayless KJ, Davis MJ, Meininger GA. Regulation of Tissue Injury Responses by the Exposure of Matricryptic Sites within Extracellular Matrix Molecules. Am J Pathol. 2000 May 1;156(5):1489–98.

113.   Li D, Zhou J, Chowdhury F, Cheng J, Wang N, Wang F. Role of mechanical factors in fate decisions of stem cells. Regen Med. 2011 Mar;6(2):229–40.

114.   Muiznieks LD, Keeley FW. Molecular assembly and mechanical properties of the extracellular matrix: A fibrous protein perspective. Biochim Biophys Acta BBA - Mol Basis Dis. 2013 Jul 1;1832(7):866–75.

115.   Costa J, Ahluwalia A. Advances and Current Challenges in Intestinal in vitro Model Engineering: A Digest. Front Bioeng Biotechnol. 2019 Jun 18;7:144.

116.   Dhillon J, Young SA, Sherman SE, Bell GI, Amsden BG, Hess DA, et al. Peptide-modified methacrylated glycol chitosan hydrogels as a cell-viability

supporting pro-angiogenic cell delivery platform for human adipose-derived stem/stromal cells. J Biomed Mater Res A. 2019;107(3):571–85.

117.   Gratzer DPF, Harrison RD, Woods T. Matrix Alteration and Not Residual Sodium Dodecyl Sulfate Cytotoxicity Affects the Cellular Repopulation of a Decellularized Matrix. :16.

118.   Zvarova B, Uhl FE, Uriarte JJ, Borg ZD, Coffey AL, Bonenfant NR, et al. Residual Detergent Detection Method for Nondestructive Cytocompatibility Evaluation of Decellularized Whole Lung Scaffolds. Tissue Eng Part C Methods. 2016 May 1;22(5):418–28.

119.   Fernández-Pérez J, Ahearne M. The impact of decellularization methods on extracellular matrix derived hydrogels. Sci Rep. 2019 Oct 17;9(1):14933.

120.   Jackson RL, Busch SJ, Cardin AD. Glycosaminoglycans: molecular properties, protein interactions, and role in physiological processes. Physiol Rev. 1991 Apr 1;71(2):481–539.

121.   Lehnert D, Wehrle-Haller B, David C, Weiland U, Ballestrem C, Imhof BA, et al. Cell behaviour on micropatterned substrata: limits of extracellular matrix geometry for spreading and adhesion. J Cell Sci. 2004 Jan 1;117(1):41–52.

122.   Liu H, Wu M, Jia Y, Niu L, Huang G, Xu F. Control of fibroblast shape in sequentially formed 3D hybrid hydrogels regulates cellular responses to microenvironmental cues. NPG Asia Mater. 2020 Jun 26;12(1):1–12.

123.   Wolf MT, Daly KA, Brennan-Pierce EP, Johnson SA, Carruthers CA, D'Amore A, et al. A hydrogel derived from decellularized dermal extracellular matrix. Biomaterials. 2012 Oct 1;33(29):7028–38.

124.   Andersen T, Auk-Emblem P, Dornish M. 3D Cell Culture in Alginate Hydrogels. Microarrays. 2015 Mar 24;4(2):133–61.

125.   Moussa L, Lapière A, Squiban C, Demarquay C, Milliat F, Mathieu N. BMP Antagonists Secreted by Mesenchymal Stromal Cells Improve Colonic Organoid Formation: Application for the Treatment of Radiation-induced Injury. Cell Transplant. 2020 Jan 1;29:0963689720929683.

126.   Nilsson T, Mann M, Aebersold R, Yates JR, Bairoch A, Bergeron JJM. Mass spectrometry in high-throughput proteomics: ready for the big time. Nat Methods. 2010 Sep;7(9):681–5.

127.   Seif-Naraghi SB, Horn D, Schup-Magoffin PJ, Christman KL. Injectable extracellular matrix derived hydrogel provides a platform for enhanced retention and delivery of a heparin-binding growth factor. Acta Biomater. 2012 Oct 1;8(10):3695–703.

Appendix A: Supplementary Data

Native   **DSI**
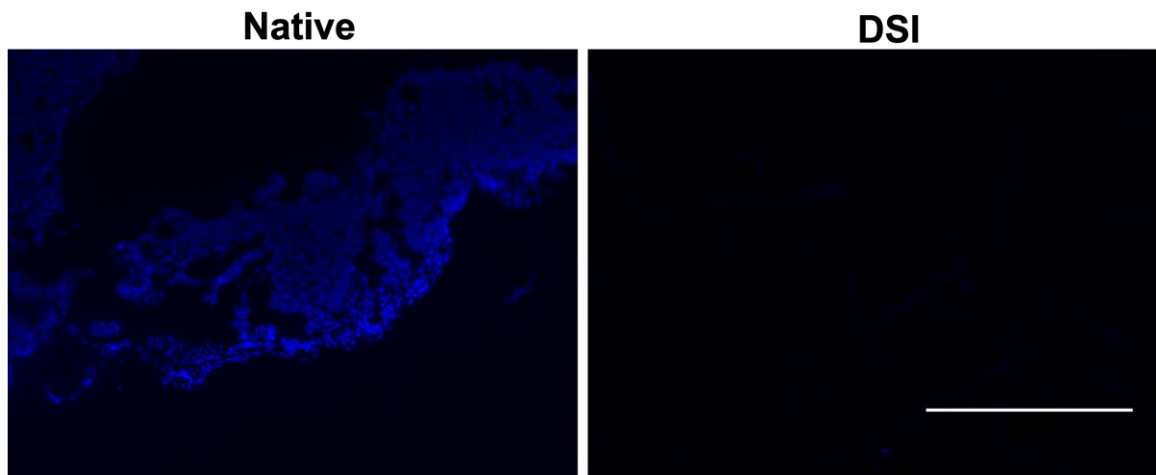
Supplementary Figure A.1. Immunofluorescence staining of native and decellularized small intestine with no primary antibody as a negative control for IHC. Representative staining showing no detectable signal (red) for any of the ECM markers in the no primary antibody control samples. No nuclei were also detected in the DSI samples through DAPI staining (blue) for cell nuclei. (n=3 cross-sections/decellularization batch, N=3 independent decellularization batches). Scale bar=400 μm.

Appendix B: Figure Permissions

THESIS COPYRIGHT PERMISSION FORM

Title(s) of the Image(s): Terese Winslow LLC owns the copyright to the following image(s):

Title(s) of illustration(s): Parts of the small intestine

Description of the Work: Terese Winslow LLC hereby grants permission to reproduce the above image(s) for use in the work specified:

Thesis title: Development of a tissue specific bioscaffold for intestinal stem cell culture

University: University of Western Ontario

Digital Object Identifier (DOI) and Journal ISSN, if available:

License Granted: Terese Winslow LLC hereby grants limited, non-exclusive worldwide print and electronic rights only for use in the Work specified. Terese Winslow LLC grants such rights "AS IS" without representation or warranty of any kind and shall have no liability in connection with such license.

Restrictions: Reproduction for use in any other work, derivative works, or by any third party by manual or electronic methods is prohibited. Ownership of original artwork, copyright, and all rights not specifically transferred herein remain the exclusive property of Terese Winslow LLC. Additional license(s) are required for ancillary usage(s).

Credit must be placed adjacent to the image(s) in the following format:

© (copyright year) Terese Winslow LLC, U.S. Govt. has certain rights

Permission granted to:
Name: Sachin Kakar
Mailing address:

Email address:
Phone number:

Signature_____ **Date**___ *2021-10-02*_____
                                   Sachin Kakar

Signature_____   Digitally signed by TERESE WINSLOW
                                                 Date: 2021.11.03 16:48:53 -04'00'   Date_____
                     Terese Winslow, CMI, Member

Terese Winslow LLC, Medical Illustration

Curriculum Vitae

Name: Sachin Kakar

Post-secondary   McMaster University
Education and   Hamilton, Ontario, Canada
Degrees: 2015-2019 B.Sc.

                       The University of Western Ontario
                       London, Ontario, Canada
                       2019-2021 M.Sc. Candidate

Honours and   Dean's Honour List at McMaster University
Awards: 2016-2019

Publications:
Josan, C., Kakar, S., & Raha, S. (2021). Matrigel® enhances 3T3-L1 cell differentiation. Adipocyte, 10(1), 361-377.

Oral Presentation at CBS-SWOSC. (2021). A novel bioscaffold for stem cell culture.

Poster Presentations at London Health Research Day. (2021). A novel bioscaffold for stem cell culture.